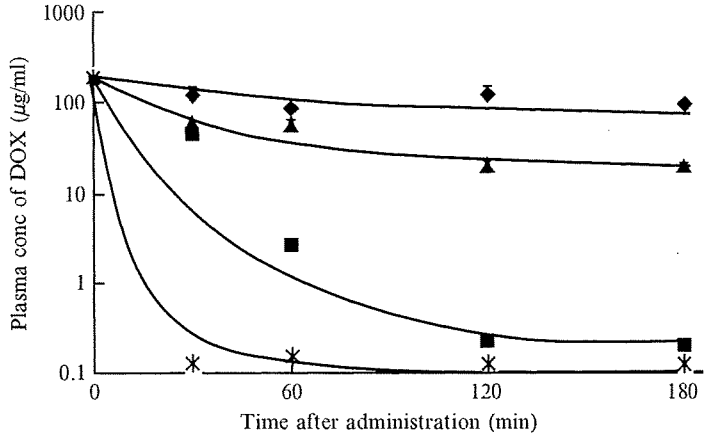

Figure 8.5 Plasma concentration of DOX. BNC–LP conjugates containing DOX (*triangles* with *solid line*), LP containing DOX (*squares* with *solid lines*), DOX alone (*crosses* with *solid lines*), and doxil (*diamonds* with *solid lines*).

be done before displaying antibodies on the surface of ZZ–BNC because antibodies displayed onto ZZ–BNC significantly reduce the fusogenic activity of ZZ–BNC (presumably by increased steric hindrance). Briefly, an aliquot of LPs (2 mg LP) containing materials of interest is gradually added to freeze-dried ZZ–BNC (100 μg as protein). We routinely add the smaller amount of antibody than ZZ–BNC (as protein) ranging from 1/5 to 1/100 (as protein) to the ZZ–BNC–LP solution. Antibodies may be spontaneously aligned on the surface of ZZ–BNC–LP conjugates by interaction of the IgG Fc domain with the ZZ domain. In the case of displaying IgG harboring weak affinity to the ZZ domain (Björck and Kronvall, 1984), a membrane-impermeable amine-reactive cross-linking agent such as bis(sulfosuccinimidyl)suberate (BS^3; Thermo Fisher Scientific, Waltham, MA, USA) was used to cross-link the binding between the IgG Fc domain and ZZ–BNC. Five millimolar BS^3 dissolved in dimethylsulfoxide (DMSO) is added to the ZZ–BNC–LP displaying IgG to a concentration of 50 μ*M*, allowed to react for 1 h, and free BS^3 removed by the reaction with 0.1 m*M* glycine. The antibody-displaying ZZ–BNC–LP conjugate is ready for *in vitro* and *in vivo* use. To our knowledge, it is not necessary to display the antibodies as much as possible onto ZZ-BNC for maximizing the delivering ability of ZZ-BNC-LP conjugate, strongly suggesting that the amounts of antibody on ZZ-BNC should be optimized in *in vitro* system.

8. Preparation of Biotin-Displaying BNC–LP Conjugates

For *in vitro* and *in vivo* retargeting of BNC–LP conjugates by various biorecognition molecules (e.g., cytokines, peptides, lectins, glycans), the surface of BNCs should be modified with these molecules without affecting fusogenic activity. The ZZ domain displayed on ZZ–BNC possesses many Lys residues, so the ε-amino residues are modified with biotin (the smallest high-affinity tag) using sulfo-biotin-NHS-ester (Thermo Fischer Scientific) according to the manufacturer's protocol. The number of biotins displayed on the surface of ZZ–BNC can be measured utilizing a 4′-hydroxyazobenzene-2-carboxylic acid (HABA) assay kit (Thermo Fisher Scientific). Usually, 1 mol of ZZ–BNC is modified with about 35 mol of biotin. Next, biotinylated ZZ–BNC–LP conjugate is mixed with an equimolar amount of biotinylated biorecognition molecules and avidins (e.g., avidin, streptavidin, neutravidin) to display the biorecognition molecules onto ZZ–BNC. As described in the antibody-displaying ZZ–BNC, the display of biorecognition molecules should be done after formation of the BNC–LP conjugate. The steric hindrance of biotinylated biorecognition molecules and avidins is too large for ZZ–BNC to exhibit fusogenic activity. The biorecognition molecules displaying the ZZ–BNC–LP conjugate is ready for *in vitro* and *in vivo* use. To our knowledge, it is not necessary to maximize the biorecognition molecules on ZZ–BNC to maximize the delivery capacity of the ZZ–BNC–LP conjugate, strongly suggesting that the amounts of biorecognition molecules on ZZ–BNC should be optimized in *in vitro* systems.

9. Concluding Remarks

The studies and methods described in this chapter demonstrate that the BNC–LP conjugate, as a hybrid of a viral vector and LPs, is a promising and rational approach to achieving a pinpoint delivery system for drugs and genes *in vivo*. Two major problems associated with BNC–LP conjugates must be resolved before they are in clinical use. The first problem is the immunogenicity of BNC–LP. BNC was initially developed as an immunogen of a recombinant hepatitis B vaccine, so BNC *per se* sometimes elicits an unexpected level of immune response. Recently, we succeeded in reducing the immunogenicity by incorporating HBV escape mutants, which can proliferate in humans vaccinated with hepatitis B vaccine. The second problem is the nonspecific incorporation by the RES. Like other nanoparticle-based medicines, BNC–LP conjugates cannot fully escape from the

RES, whereas HBV can accomplish the escape. We must analyze the endogenous escape mechanism of HBV at the molecular level, and introduce it to BNC–LP conjugates.

ACKNOWLEDGMENTS

The authors thank Professor M. Seno (Okayama University), Professor A. Kondo (Kobe University), and Professor M. Ueda (Keio University) for their helpful advice. We are grateful to Ms. Y. Matsushita, Ms. N. Shikaku, and Ms. Y. Matsui for their technical support. This work was supported in part by the Regional Research and Development Resources Utilization Program from the Japan Science and Technology Agency.

REFERENCES

Bangham, A. D., and Horne, R. W. (1964). Negative staining of phospholipids and their structural modification by surface-active agents as observed in the electron microscope. *J. Mol. Biol.* **8,** 660–668.

Batzri, S., and Korn, E. D. (1973). Single bilayer liposomes prepared without sonication. *Biochim. Biophys. Acta* **298,** 1015–1019.

Björck, L., and Kronvall, G. (1984). Purification and some properties of streptococcal protein G, a novel IgG-binding reagent. *J. Immunol.* **133,** 969–974.

Düzgüneş, N., Simões, S., Pires, P., and Pedroso de Lima, M. C. (2002). Gene delivery by cationic liposome-DNA complexes. *In* "Polymeric Biomaterials," (S. Dumitriu, ed.), pp. 943–958. Marcel Dekker, New York.

Glebe, D., and Urban, S. (2007). Viral and cellular determinants involved in hepadnaviral entry. *World J. Gastroenterol.* **13,** 22–38.

Hama, S., Akita, H., Ito, R., Mizuguchi, H., Hayakawa, T., and Harashima, H. (2006). Quantitative comparison of intracellular trafficking and nuclear transcription between adenoviral and lipoplex systems. *Mol. Ther.* **13,** 786–794.

Hinnen, A., Hicks, J. B., and Fink, G. R. (1978). Transformation of yeast. *Proc. Natl. Acad. Sci. USA* **75,** 1929–1933.

Hong, R. L., Huang, C. J., Tseng, Y. L., Pang, V. F., Chen, S. T., Liu, J. J., and Chang, F. H. (1999). Direct comparison of liposomal doxorubicin with or without polyethylene glycol coating in C-26 tumor-bearing mice: Is surface coating with polyethylene glycol beneficial? *Clin. Cancer Res.* **5,** 3645–3652.

Iwasaki, Y., Ueda, M., Yamada, T., Kondo, A., Seno, M., Tanizawa, K., Kuroda, S., Sakamoto, M., and Kitajima, M. (2007). Gene therapy of liver tumors with human liver-specific nanoparticles. *Cancer Gene Ther.* **14,** 74–81.

Jung, J., Matsuzaki, T., Tatematsu, K., Okajima, T., Tanizawa, K., and Kuroda, S. (2008). Bio-nanocapsule conjugated with liposomes for *in vivo* pinpoint delivery of various materials. *J. Control. Release* **126,** 255–264.

Kasuya, T., and Kuroda, S. (2009). Nanoparticles for human liver-specific drug and gene delivery systems: *In vitro* and *in vivo* advances. *Expert Opin. Drug Deliv.* **6,** 39–52.

Kasuya, T., Nomura, S., Matsuzaki, T., Jung, J., Yamada, T., Tatematsu, K., Okajima, T., Tanizawa, K., and Kuroda, S. (2008a). Expression of squamous cell carcinoma antigen-1 in liver enhances the uptake of hepatitis B virus envelope-derived bio-nanocapsules in transgenic rats. *FEBS J.* **275,** 5714–5724.

Kasuya, T., Yamada, T., Uyeda, A., Matsuzaki, T., Okajima, T., Tatematsu, K., Tanizawa, K., and Kuroda, S. (2008b). *In vivo* protein delivery to human liver-derived cells using hepatitis B virus envelope pre-S region. *J. Biosci. Bioeng.* **106,** 99–102.

Kasuya, T., Jung, J., Kadoya, H., Matsuzaki, T., Tatematsu, K., Okajima, T., Miyoshi, E., Tanizawa, K., and Kuroda, S. (2008c). *In vivo* delivery of bionanocapsules displaying *Phaseolus vulgaris* agglutinin-L_4 isolectin to malignant tumors overexpressing *N*-acetylglucosaminyltransferase V. *Hum. Gene Ther.* **19,** 887–895.

Kikuchi, A., Aoki, Y., Sugaya, S., Serikawa, T., Takakuwa, K., Tanaka, K., Suzuki, N., and Kikuchi, H. (1999). Development of novel cationic liposomes for efficient gene transfer into peritoneal disseminated tumor. *Hum. Gene Ther.* **10,** 947–955.

Kobayashi, M., Asano, T., Utsunomiya, M., Itoh, Y., Fujisawa, Y., Nishimura, O., Kato, K., and Kakinuma, A. (1988). Recombinant hepatitis B virus surface antigen carrying the pre-S2 region derived from yeast: Purification and characterization. *J. Biotechnol.* **8,** 1–22.

Kurata, N., Shishido, T., Muraoka, M., Tanaka, T., Ogino, C., Fukuda, H., and Kondo, A. (2008). Specific protein delivery to target cells by antibody-displaying bionanocapsules. *J. Biochem.* **144,** 701–707.

Kuroda, S., Otaka, S., Miyazaki, T., Nakao, M., and Fujisawa, Y. (1992). Hepatitis B virus envelope L protein particles. Synthesis and assembly in *Saccharomyces cerevisiae*, purification and characterization. *J. Biol. Chem.* **267,** 1953–1961.

Lasic, D., and Martin, F. (eds.) (1995). *In* "Stealth Liposomes", CRC Press, Boca Raton, FL.

Li, S. D., and Huang, L. (2006). Gene therapy progress and prospects: Non-viral gene therapy by systemic delivery. *Gene Ther.* **13,** 1313–1319.

Lorusso, V., Manzione, L., and Silvestris, N. (2007). Role of liposomal anthracyclines in breast cancer. *Ann. Oncol.* **18,** 70–73.

Maeda, H., Wu, J., Sawa, T., Matsumura, Y., and Hori, K. (2000). Tumor vascular permeability and the EPR effect in macromolecular therapeutics: A review. *J. Control. Release* **65,** 271–284.

Markman, M. (2006). Pegylated liposomal doxorubicin in the treatment of cancers of the breast and ovary. *Expert Opin. Pharmacother.* **7,** 1469–1474.

Marshall, E. (2002). Clinical research. Gene therapy a suspect in leukemia-like disease. *Science* **298,** 34–35.

Moghimi, S. M., and Szebeni, J. (2003). Stealth liposomes and long circulating nanoparticles: Critical issues in pharmacokinetics, opsonization and protein-binding properties. *Prog. Lipid Res.* **42,** 463–478.

Moghimi, S. M., Hunter, A. C., and Murray, J. C. (2001). Long-circulating and target-specific nanoparticles: Theory to practice. *Pharmacol. Rev.* **53,** 283–318.

Nagaoka, T., Fukuda, T., Yoshida, S., Nishimura, H., Yu, D., Kuroda, S., Tanizawa, K., Kondo, A., Ueda, M., Yamada, H., Tada, H., and Seno, M. (2007). Characterization of bio-nanocapsule as a transfer vector targeting human hepatocyte carcinoma by disulfide linkage modification. *J. Control. Release* **118,** 348–356.

Parr, M. J., Masin, D., Cullis, P. R., and Bally, M. B. (1997). Accumulation of liposomal lipid and encapsulated doxorubicin in murine Lewis lung carcinoma: the lack of beneficial effects by coating liposomes with poly(ethylene glycol). *J. Pharmacol. Exp. Ther.* **280,** 1319–1327.

Richardson, M. (2006). AmBisome: Adds to the body of knowledge and familiarity of use. *Acta Biomed.* **77,** 3–11.

Rosenthal, E., Poizot-Martin, I., Saint-Marc, T., Spano, J. P., and Cacoub, P.DNX Study Group (2002). Phase IV study of liposomal daunorubicin (DaunoXome) in AIDS-related Kaposi sarcoma. *Am. J. Clin. Oncol.* **25,** 57–59.

Savulescu, J. (2001). Harm, ethics committees and the gene therapy death. *J. Med. Ethics* **27,** 148–150.

Szoka, F. Jr., and Papahadjopoulos, D. (1978). Procedure for preparation of liposomes with large internal aqueous space and high capture by reverse-phase evaporation. *Proc. Natl. Acad. Sci. USA* **75,** 4194–4198.

Takayama, M., Itoh, S., Nagasaki, T., and Tanimizu, I. (1977). A new enzymatic method for determination of serum choline-containing phospholipids. *Clin. Chim. Acta* **79,** 93–98.

Tsutsui, Y., Tomizawa, K., Nagita, M., Michiue, H., Nishiki, T., Ohmori, I., Seno, M., and Matsui, H. (2007). Development of bionanocapsules targeting brain tumors. *J. Control. Release* **122,** 159–164.

Yamada, T., Iwabuki, H., Kanno, T., Tanaka, H., Kawai, T., Fukuda, H., Kondo, A., Seno, M., Tanizawa, K., and Kuroda, S. (2001). Physicochemical and immunological characterization of hepatitis B virus envelope particles exclusively consisting of the entire L (pre-S1 + pre-S2 + S) protein. *Vaccine* **19,** 3154–3163.

Yamada, T., Iwasaki, Y., Tada, H., Iwabuki, H., Chuah, M. K., VandenDriessche, T., Fukuda, H., Kondo, A., Ueda, M., Seno, M., Tanizawa, K., and Kuroda, S. (2003). Nanoparticles for the delivery of genes and drugs to human hepatocytes. *Nat. Biotechnol.* **21,** 885–890.

Yu, D., Amano, C., Fukuda, T., Yamada, T., Kuroda, S., Tanizawa, K., Kondo, A., Ueda, M., Yamada, H., Tada, H., and Seno, M. (2005). The specific delivery of proteins to human liver cells by engineered bio-nanocapsules. *FEBS J.* **272,** 3651–3660.

Integrin signal masks growth-promotion activity of HB-EGF in monolayer cell cultures

Hiroto Mizushima[1], Xiaobiao Wang[1], Shingo Miyamoto[2] and Eisuke Mekada[1,*]

[1]Department of Cell Biology, Research Institute for Microbial Diseases, Osaka University, 3-1 Yamadaoka, Suita, Osaka 565-0871, Japan
[2]Department of Obstetrics and Gynecology, School of Medicine, Fukuoka University, 7-45-1 Nanakuma, Fukuoka 814-0180, Japan
*Author for correspondence (emekada@biken.osaka-u.ac.jp)

Accepted 11 September 2009
Journal of Cell Science 122, 4277-4286 Published by The Company of Biologists 2009
doi:10.1242/jcs.054551

Summary

The extracellular environment and tissue architecture contribute to proper cell function and growth control. Cells growing in monolayers on standard polystyrene tissue culture plates differ in their shape, growth rate and response to external stimuli, compared with cells growing in vivo. Here, we showed that the EGFR (epidermal growth factor receptor) ligand heparin-binding EGF-like growth factor (HB-EGF) strongly stimulated cell growth in nude mice, but not in cells cultured in vitro. We explored the effects of HB-EGF on cell growth under various cell culture conditions and found that growth promotion by HB-EGF was needed in three-dimensional (3D) or two-dimensional (2D) culture systems in which cell-matrix adhesion was reduced. Under such conditions, cell growth was extremely suppressed in the absence of HB-EGF, but markedly potentiated in the presence of HB-EGF. When the integrin signal was reduced using antibodies or knockout of either integrin β1 or focal adhesion kinase (FAK), cells showed HB-EGF-dependent growth. We also showed that EGF, transforming growth factor-α (TGFα) or ligands of other receptor tyrosine kinases (RTKs) stimulated cell growth in 3D culture, but not in tissue culture plates. These results indicate that the integrin signal was sufficient to support cell growth in 2D tissue culture plates without addition of the growth factor, whereas stimulation by growth factors was clearly demonstrated in culture systems in which integrin signals were attenuated.

Supplementary material available online at
http://jcs.biologists.org/cgi/content/full/122/23/4277/DC1

Key words: EGFR, HB-EGF, Integrin, 3D culture

Introduction

Establishment of cell culture methods of mammalian cells stimulated revolutionary progress in biology and medicine, and has now become an essential technology in cell biology research. Mammalian cell culture is most commonly achieved by incubating cells with a defined nutrient medium supplemented with serum in tissue culture plates. Cells attach and adhere onto the flat surface of glass or plastic plates and grow two dimensionally, forming monolayer sheets. Although the standard cell culture system has provided us with fundamental knowledge of cell and gene functions, this system is not an accurate representation of the in vivo environment in which the cells originally exist (Lee et al., 2007; Schmeichel and Bissell, 2003; Yamada and Cukierman, 2007). Tissues and organs are three-dimensional (3D). Cells grown on flat tissue culture plates (TCPs) using standard cell culture methods differ from those growing in their natural environments in terms of their morphology, physicochemical properties of the substrate they attach to, and cell-cell and cell-matrix interactions. Thus, the behavior, growth and differentiation, as well as their response to internal and external signals, of cells grown in the standard cell culture environments are largely different to that of cells grown in vivo.

The EGFR-ligand system supports the proliferation, motility, differentiation and survival of various cell types, thereby contributing to the development, morphogenesis and maintenance of homeostasis in the body. The EGF-EGFR system also has a pivotal role in the progression and development of malignant tumor growth (Hynes and Lane, 2005; Normanno et al., 2006; Lynch et al., 2004; Paszek et al., 2005). Furthermore, the overexpression of EGFR ligands induces or enhances cell growth in nude mice (Miyamoto et al., 2004; Ongusaha et al., 2004; Wang et al., 2006; Normanno et al., 2006). However, in contrast to the marked effects of EGFR ligands on tumor cell growth in vivo, the growth-promoting properties of the EGFR ligands have not been well documented in most cell types using standard cell culture methods. Early studies indicated that EGF increased the lifetime, but not the growth rate, of primary keratinocytes in culture (Rheinwald and Green, 1977). Previous studies using normal keratinocytes, fibroblasts, breast cancer cells and neuroblastoma cells reported that EGFR ligands stimulated cell growth with a minimal increase in cell numbers (Hashimoto et al., 1994; Ho et al., 2005; Lembach, 1976; Osborne et al., 1980). Moreover, in some cases, EGFR ligands induced cell-cycle arrest or apoptosis (Cao et al., 2000; Fan et al., 1995). Even under serum-depleted conditions, the addition of growth factors to the cell culture medium resulted in only a slight growth promotion, if any. The lack of an appropriate in vitro culture system to demonstrate growth promotion by EGFR ligands posed a limitation in understanding the signaling mechanism and molecules responsible for the proliferating effect of these growth factors. The exceptions are the myeloid lineage cell lines 32D and Ba/F3. These cell lines, which normally grow in suspension in an interleukin-3-dependent manner, can proliferate specifically in response to EGFR ligands by expressing ectopic EGFR in the absence of interleukin-3, thus facilitating observation of its growth-promotion activity (Higashiyama et al., 1995; Iwamoto et al., 1999; Pierce et al., 1988; Yu et al., 2002). These findings suggest that cellular responses to EGFR ligands vary according to the cell culture conditions and cell systems used for the study. However, the reason

for this low potency of EGFR ligands in most cell types has not been investigated in much detail.

HB-EGF is an essential member of the EGFR ligands in vivo, which is synthesized as a transmembrane precursor protein (proHB-EGF) (Higashiyama et al., 1991). Its extracellular domain is then cleaved by proteases, via a so-called ectodomain-shedding mechanism, which yields a soluble mature growth factor (sHB-EGF), which is similar to other EGFR ligands (Goishi et al., 1995; Massagué and Pandiella, 1993). In the course of the present study, we found that HB-EGF did not promote the growth of ovarian cancer cell lines under standard monolayer cell culture conditions, although it enhanced the cell growth rates when the same cell lines were injected into nude mice. Thus, we focused on the growth-stimulatory effect of HB-EGF under various culture conditions and found that this effect of HB-EGF was not well documented in the standard monolayer culture. However, it was particularly observed in culture systems in which the integrin signal was attenuated. We also show that such culture conditions enable the observation of cell proliferation by EGF, TGFα or ligands of other receptor tyrosine kinases (RTKs). The results of the present study indicate why the growth-promotion activity of growth factors has thus far not been well documented in vitro.

Results

HB-EGF promotes cell growth in vivo but not in vitro

We previously reported that the tumorigenicity of the ovarian cancer cell lines SKOV3 and RMG-1 when injected into nude mice were strongly enhanced by exogenous expression of HB-EGF, whereas small-hairpin RNA-mediated knockdown of endogenous HB-EGF or administration of the HB-EGF-specific inhibitor CRM197 suppressed their tumorigenicities (Miyamoto et al., 2004). We confirmed the contribution of HB-EGF to SKOV3 cell growth in vivo by overexpression or knockdown experiments (Fig. 1A). Although the tumorigenic growth of xenografted cells might be affected by various host factors, the marked growth-promotion effect of HB-EGF in vivo led to the proposal that HB-EGF also contributes to SKOV3 cell growth in vitro. To test this hypothesis, we compared the growth rates of SKOV3 cells, HB-EGF-overexpressing SKOV3 (SKOV-HB) cells and HB-EGF-knockdown SKOV3 cells under monolayer culture conditions using standard polystyrene tissue culture plates (TCPs). Contrary to our expectation, no obvious differences in the growth rates between the parental and HB-EGF-overexpressing SKOV3 cells in TCPs were observed (Fig. 1A). Moreover, SKOV3 cells expressing small-hairpin RNAs specific for HB-EGF, which had lost their tumorigenicity, were able to grow almost as quickly as the parental cells in TCPs (Fig. 1A).

To further study the effects of HB-EGF on cell growth, we used BRL cells, which are originally non-tumorigenic and become tumorigenic upon HB-EGF overexpression (Wang et al., 2006). We established BRL cells overexpressing wild-type HB-EGF (BRL-HB) or an ectodomain-shedding deficient mutant HB-EGF (BRL-HBuc) (Miyamoto et al., 2004; Yamazaki et al., 2003), and compared their growth rates with that of mock virus-infected BRL cells (BRL-mock). Although BRL-HB and BRL-HBuc cells expressed comparable amounts of the HB-EGF precursor (proHB-EGF), the secretion of sHB-EGF by BRL-HBuc cells was significantly reduced compared with that of BRL-HB cells (supplementary material Fig. S1). When BRL-HB cells were subcutaneously injected into nude mice they formed tumors, as reported previously (Wang et al., 2006). However, neither BRL-HBuc cells nor BRL-mock cells formed tumors until 3 weeks after injection (Fig. 1B). Similarly to SKOV3 cells, these cells grew at comparable rates in TCPs (Fig. 1B). These results indicated that HB-EGF promotes the growth of non-tumorigenic cells in vivo in an ectodomain-shedding-dependent manner, although HB-EGF did not potentiate cell growth in cells grown using in vitro culture conditions.

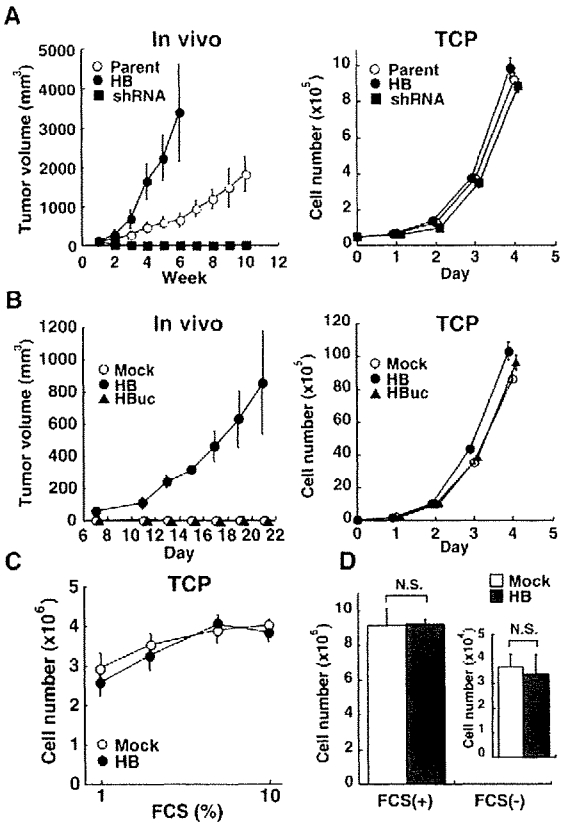

Fig. 1. Effects of HB-EGF on cell growth. (A) Tumorigenicity in vivo and growth of SKOV3 cells in TCPs. SKOV3 cells (Parent), SKOV3-HB cells (HB) or overexpressing small-hairpin RNAs for HB-EGF (shRNA) were injected into nude mice (n=16) or cultured in TCPs. The mean tumor volume (± s.d.) and cell number were determined. SKOV3 cells, SKOV-HB cells or SKOV3 cells expressing small-hairpin RNAs for HB-EGF were grown in TCPs. (B) Tumorigenicity in vivo and growth of BRL cells in TCPs. BRL cells (Mock), BRL-HB cells (HB) or BRL-HBuc cells (HBuc) were injected into nude mice (n=4) or cultured in TCPs. The mean tumor volume and cell number were determined. (C) Effect of FCS on BRL cell growth in TCPs. BRL cells (Mock) or BRL-HB cells (HB) were cultured with medium containing various concentrations of FCS for 4 days and cell number was counted. (D) Effects of HB-EGF on cell growth under FCS-free conditions. BRL cells (Mock) or BRL-HB cells (HB; 5×10^4) were cultured with FCS-containing or FCS-free defined medium for 4 days. Result for FCS-free defined medium is also shown in inset. N.S., not significant.

All the cultures described above were performed in medium containing 10% FCS. We tested the effect of serum on the growth-stimulating effect of HB-EGF in TCPs. Even in medium containing 1% FCS, the cells grew as quickly as those cultured in medium containing 10% serum; HB-EGF did not potentiate their growth rate (Fig. 1C). To rule out any effects of serum, cells were cultured using a serum-free defined medium as described in the Materials and Methods. Overall, the growth rate of BRL and SKOV3 cells,

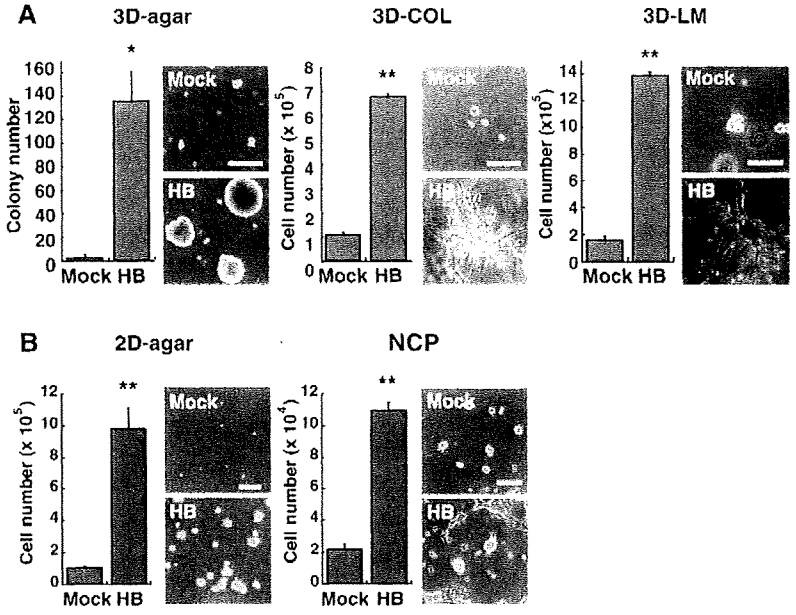

Fig. 2. Growth of BRL cells under various culture conditions. BRL cells (Mock) or BRL-HB cells (HB) were cultured under 3D culture conditions (A) or 2D culture conditions (B). (A) Cells were cultured in 3D-agar for 4 weeks, 3D-COL for 1 week or 3D-LM for 4 days. (B) Cells were cultured onto soft agar (2D-agar) for 1 week or NCPs for 3 days. Representative morphologies of BRL-mock and BRL-HB cells grown in 3D-agar (scale bar: 200 μm), 3D-COL (scale bar: 100 μm), 3D-LM (scale bar: 250 μm), 2D-agar (scale bar: 250 μm) or NCPs (scale bar: 250 μm) are shown. All cell cultures were maintained in the presence of FCS. *P<0.02, **P<0.01.

regardless of HB-EGF expression, was largely reduced under serum-free conditions. Even in the serum-free medium, HB-EGF did not enhance BRL (Fig. 1D) and SKOV3 cell growth (supplementary material Fig. S2).

To test whether the inability of HB-EGF to enhance cell growth in TCPs was a common feature, we tested the effect of HB-EGF on cell growth in three other cell lines, A431, RMG-1 and U373 MG cells. Similarly to BRL and SKOV3 cells, the exogenous expression of HB-EGF did not increase the growth rates of A431, RMG-1 and U373 MG cells in TCPs, either in medium containing 10% FCS or in serum-free defined medium (supplementary material Fig. S3). These results suggest that the inability of HB-EGF to promote growth in TCPs is not attributable to the existence of FCS in the culture medium.

HB-EGF enhances cell growth under 3D culture conditions

Tumorigenic cells can often grow in semisolid media, such as soft agar (Hanahan and Weinberg, 2000). HB-EGF induces oncogenic transformation in several cell lines and confers the ability to grow in soft agar (Fu et al., 1999; Harding et al., 1999; Ongusaha et al., 2004). Consistently with previous studies, HB-EGF strongly potentiated BRL cell growth in the presence of 10% FCS in soft agar (hereafter cell culture in soft agar is referred to as 3D-agar). BRL-HB cells grew to form spherical colonies in 3D-agar, but BRL-mock cells did not (Fig. 2A). One characteristic difference between cell culture conditions in 3D-agar and 2D plates is that cells embedded in gels grow three-dimensionally (in a multilayer). Therefore, we examined whether BRL cells grew in an HB-EGF-dependent manner under other 3D culture conditions. 3D cultures consisted of 3D matrices, such as collagen gels (hereafter referred to as 3D-COL) or a laminin-rich matrix (hereafter referred to as 3D-LM) (Paszek et al., 2005; Weaver et al., 1997). Although the morphology of BRL-HB cells growing in 3D-COL and 3D-LM was different to that in 3D-agar, HB-EGF markedly enhanced cell proliferation in these 3D cultures (Fig. 2A). In 3D-COL, BRL-mock cells proliferated to twice their initial number, whereas BRL-HB cells proliferated rapidly and increased their numbers around seven times faster than BRL-mock cells after 1 week of culture. BRL-HB cells proliferated even more rapidly in 3D-LM than in 3D-COL and multiplied around seven times faster than BRL-mock cells after 4 days of culture (Fig. 2A). Growth enhancement by HB-EGF in 3D culture conditions was observed for SKOV3, A431, RMG-1 and U373 MG cells (supplementary material Figs S2, S3).

In the above experiments, proHB-EGF was overexpressed in BRL cells and other cell lines to examine the effect of HB-EGF on cell growth. We also performed similar experiments by adding recombinant sHB-EGF to the medium as an alternative to proHB-EGF overexpression. sHB-EGF promoted the growth of BRL-mock cells in a dose-dependent manner in 3D-COL, but not in TCPs (supplementary material Fig. S4A). HB-EGF-dependent growth was also tested using MCF-10A, another non-transformed cell line. The addition of sHB-EGF induced a ~3.5-fold increase in growth of MCF-10A cells in 3D-LM, but weakly induced (~1.3-fold) growth of the cells in TCPs (supplementary material Fig. S4B). These results indicate that growth promotion by HB-EGF in 3D cultures is a general phenomenon observed for transformed and non-transformed cells, and that HB-EGF-dependent growth in 3D cultures is reflected by both the overexpression of proHB-EGF and by addition of sHB-EGF in the medium.

CRM197, a specific inhibitor of HB-EGF, suppresses HB-EGF-dependent growth of ovarian cancer cell lines in vivo (Miyamoto et al., 2004). CRM197 did not affect the growth of BRL-mock and BRL-HB cells in TCPs (supplementary material Fig. S5). In 3D-COL, however, CRM197 suppressed the growth of BRL-HB, but not BRL-mock cells, further confirming HB-EGF-dependent growth in 3D-COL (supplementary material Fig. S5).

HB-EGF enhances cell growth under 2D reduced cell adhesion conditions

As shown above, the growth enhancement by HB-EGF was clearly observed in 3D culture systems in which cells were embedded either into a soft agar, collagen or laminin-rich matrix. To determine whether the embedding of cells into the gel was critically required for cell growth enhancement by HB-EGF, we tested other cell

culture conditions: (1) cells were cultured atop a soft agar surface (2D-agar); (2) cells were cultured on NanoCulture® plates (NCPs). We compared the growth rate of BRL-HB cells with those of BRL-mock cells grown under these culture conditions. When BRL cells were cultured in 2D-agar, cell adhesion and spreading were strongly suppressed. Under these conditions, BRL-mock cells scarcely grew, but BRL-HB cells proliferated and formed spheroidal cell masses (Fig. 2B). NCPs with a nanometer scale honeycomb-patterned structure on the surface are shown to reduce cell adhesion to the matrix (http://www.scivax.com/cell/english/index.html). In NCPs, cell adhesion, spreading and monolayer cell sheet formation were hampered in the case of BRL cells, and these cells showed HB-EGF-dependent growth (Fig. 2B).

Cells embedded in gels might differ from cells growing in TCPs largely because of their surrounding microenvironments. In 3D, for example, gas exchange, nutrient supply and diffusion of growth factors might be hampered, compared with TCPs. However, since growth promotion by HB-EGF was observed to be as high as that of 3D culture conditions using 2D-agar or NCP, the difference of these factors might not be critical in determining the requirement of HB-EGF for cell growth. It was interesting that growth enhancement by HB-EGF was observed in reduced cell-matrix adhesion conditions, as seen in 2D-agar and NCPs, whereas HB-EGF-dependent cell growth was not observed in TCPs, which allow cells to attach, spread and form monolayers.

Growth rates of cells cultured in 3D or reduced cell adhesion conditions are much lower than those cultured in TCPs

To characterize the conditions that facilitate growth promotion by HB-EGF, we examined the growth rates of BRL cells under various culture conditions. For this experiment, methylcellulose gel was used instead of soft agar for the 3D-agar condition for the ease of cell counting (therefore referred to as 3D-MC). Since cell growth rate was different in each culture condition, cell number was counted at distinct culture periods. The growth curve of BRL-mock and BRL-HB cells in TCPs and 3D-COL are shown in Fig. 3A. Cell numbers of BRL-mock and BRL-HB cells cultured in NCP, 3D-LM, 2D-agar and 3D-MC for the days indicated are also shown in Fig. 3B. These results indicate that the growth rate of cells in TCPs is extremely high compared with that of other culture conditions in vitro. Based on Fig. 3A and 3B, we also examined the relationship of the 'growth rate' of BRL cells without HB-EGF and the 'upregulation ratio' by HB-EGF. The growth rate was estimated by comparison of the doubling time of BRL-mock cells in various culture conditions without HB-EGF, and the upregulation ratio was estimated by comparison of growth rate between BRL-mock and BRL-HB cells, as described in the Materials and Methods. Fig. 3C shows the relationship of the growth rate and upregulation ratio in each culture condition. The cells in culture conditions with lower growth rates showed a higher upregulation ratio, although this was not the case for 3D-MC. Thus, the enhancement of cell growth by HB-EGF was particularly observed in culture conditions in which overall cell growth was reduced.

HB-EGF enhances cell growth in 3D culture by activating Raf-MEK-Erk and PI3K-Akt pathways

We examined which EGFR downstream signaling molecules were responsible for cell growth in TCPs and 3D-COL upon HB-EGF stimulation. BRL-HB cell growth in 3D-COL was suppressed by inhibitors of EGFR (ZD1839), MEK (PD98059) and phosphatidylinositol-3 kinase (PI3K; LY294002), but not ErbB2

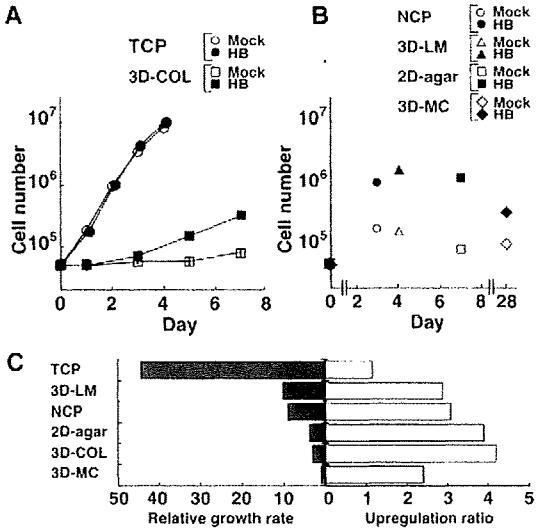

Fig. 3. Negative correlation between growth rate and HB-EGF dependency. (A) Growth curve of BRL cells (Mock) and BRL-HB cells (HB) in TCPs or 3D-COL. (B) Growth of BRL cells (Mock) and BRL-HB cells (HB) in NCP, 2D-agar, 3D-LM or 3D-MC. The numbers of cells was counted at indicated periods. (C) Relative growth rates and upregulation ratios under various culture conditions. Cell growth rates relative to that in 3D-MC and upregulation ratios by HB-EGF in various culture conditions.

(AG825) or p38MAPK (SB203580; Fig. 4A). This suggested that EGFR and its downstream MEK-Erk and PI3K-Akt signals were required for BRL-HB cell growth in 3D-COL. The PI3K inhibitor LY294002 inhibited BRL-HB cells in TCPs as well as in 3D-COL. Kinetic studies with increasing concentrations of inhibitors indicated that BRL-HB cell growth was largely suppressed by the MEK inhibitor PD98059 in 3D-COL and partially suppressed in TCPs within a higher concentration range (Fig. 4B). These findings suggest that MEK and PI3K are required for cell growth in TCPs as well as 3D-COL, but cells grown in 3D-COL were more susceptible to the inhibitors than cells grown in TCPs.

HB-EGF-dependent cell growth in 3D-COL was suppressed by inhibitors of MEK or PI3K, suggesting that activation of the Raf-MEK-Erk and PI3K-Akt pathways is crucial for promoting cell growth. To test whether activation of these pathways could substitute for the activity of HB-EGF, wild-type Raf-1, MEK1 and Akt1 were overexpressed in BRL-mock cells. Raf-1 alone, MEK1 alone or Raf-1 plus MEK1 did not significantly promote cell growth, whereas Akt1 alone partially promoted cell growth (data not shown). However, coexpression of Raf-1, MEK1 and Akt1, induced BRL cells to change their morphology to that resembling BRL-HB cells and promoted cell growth at comparable levels to those induced by HB-EGF (Fig. 4C), suggested that the coordinated activation of the Raf-MEK-Erk and PI3K-Akt pathways was crucial for potentiating cell growth in 3D-COL. By contrast, cell growth was not significantly affected by coexpression of Raf-1, MEK1 and Akt1 in TCPs (Fig. 4C). These results indicate that HB-EGF enhanced cell growth in 3D culture by activating both the Raf-MEK-Erk and PI3K-Akt pathways.

Attenuation of EGFR and its downstream signaling is associated with HB-EGF dependency

Next, we examined the activation states of EGFR, Erk and Akt in cells grown in TCPs and 3D-COL before and after transient HB-

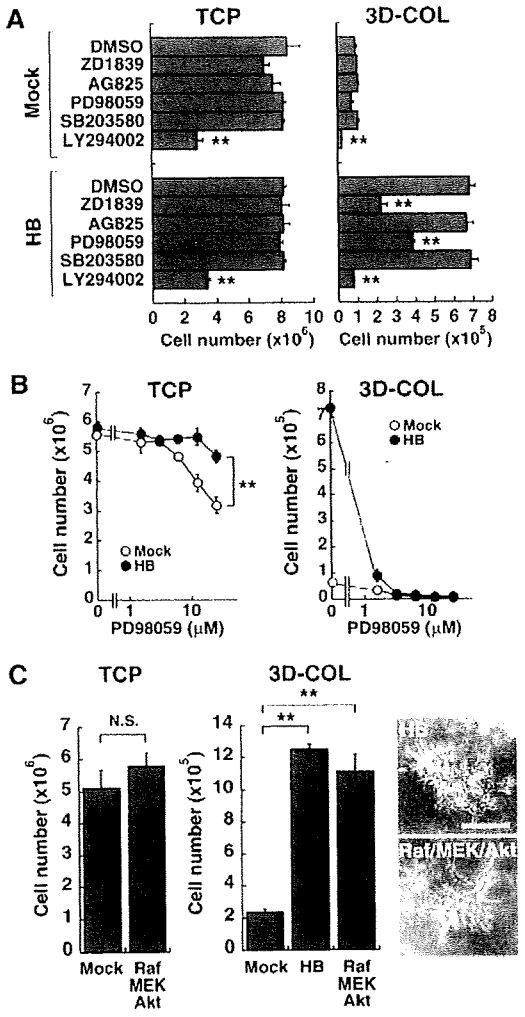

Fig. 4. Signaling pathways required for HB-EGF-dependent cell growth. (A) Effects of various kinase inhibitors on the growth of BRL cells. BRL-mock and BRL-HB cells were cultured in the presence of vehicle (DMSO) or the following kinase inhibitors: ZD1839 (100 nM), EGFR inhibitor; AG825 (100 nM), ErbB2 inhibitor; PD98059 (1 μM), MEK inhibitor; SB203580 (1 μM), p38MAPK inhibitor; or LY294002 (10 μM), PI3K inhibitor. (B) Effects of the MEK inhibitor on cell growth. Cells were grown in the presence of the indicated concentrations of PD98059. (C) Cooperation of Raf-1, MEK1 and Akt1. BRL-mock cells, BRL-HB cells or BRL cells expressing Raf-1, MEK1 and Akt1 were grown in TCPs for 4 days or 3D-COL for 1 week. Representative images of cells grown in 3D-COL are shown. All cell cultures were maintained in the presence of 10% FCS. N.S., not significant; $^{**}P<0.01$. Scale bar: 50 μm.

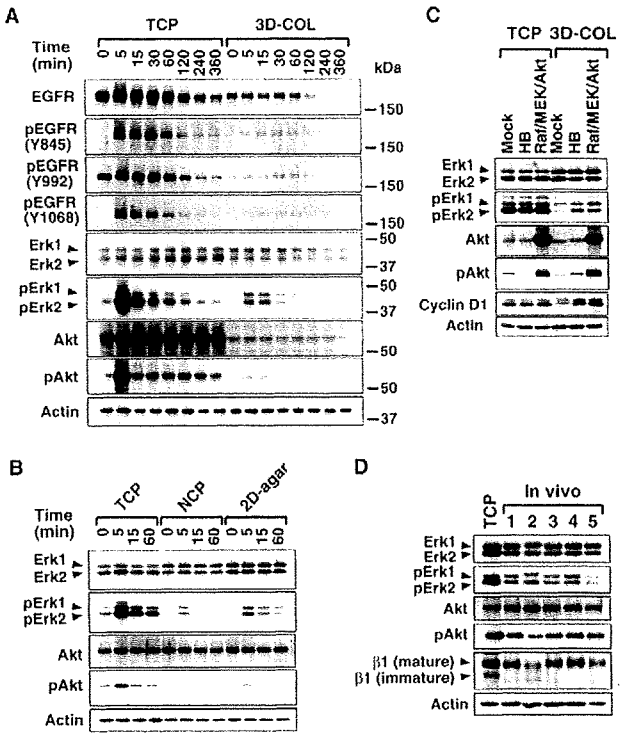

Fig. 5. Activation states of EGFR and its downstream pathways. (A) Transient activation of EGFR signaling in 3D-COL. BRL-mock cells were pre-cultured for 16 hours in the presence of 1% FCS in TCPs or 3D-COL, and then stimulated with recombinant sHB-EGF (30 ng/ml) for the indicated periods. Activation of EGFR, Erk and Akt was monitored using their phospho-specific antibodies. Actin was used as a control. (B) Transient activation of EGFR downstream pathways in 2D cell adhesion-reduced conditions. BRL-mock cells were pre-cultured for 16 hours in the presence of 1% FCS in NCPs or 2D-agar, and then stimulated with recombinant sHB-EGF (30 ng/ml) for the indicated periods. (C) Steady-state activation of EGFR downstream pathways. BRL-mock cells, BRL-HB cells and BRL cells expressing Raf-1, MEK1 and Akt1 were grown in TCPs or 3D-COL for 4 days in the presence of 10% FCS. Activation of Erk and Akt was monitored using their phospho-specific antibodies. Cell cycle was monitored with anti-cyclin-D1 antibody. Actin was used as a loading control. (D) Activation states of EGFR downstream pathways and the level of integrin β1 in vivo. BRL-HB cells were grown in TCPs for a day or nude mice for 3 weeks. Activation of Erk and Akt was monitored using their phospho-specific antibodies. Integrin β1 levels were monitored with anti-integrin β1 antibody. Actin was used as a control.

EGF stimulation. We first compared the steady-state levels of EGFR, Erk and Akt proteins of BRL cells cultured for 16 hours without sHB-EGF. The levels of EGFR and Akt proteins were markedly reduced in cells grown in 3D-COL compared with those grown in TCPs (Fig. 5A, see lanes Time 0). The Erk2, but not the Erk1 levels, were also slightly reduced in 3D-COL. Consistent with the reduction in the level of EGFR, the phosphorylation of EGFR (Y845 and Y992), Akt and Erk before HB-EGF stimulation was reduced in 3D-COL. These results indicate that the activation states of EGFR and downstream signaling molecules in the absence of HB-EGF in 3D-COL were lower compared with those in TCPs. Upon stimulation by addition of recombinant sHB-EGF, the phosphorylation levels of EGFR (Y845, Y992 and Y1068), Akt and Erk in TCPs were significantly enhanced. Although the phosphorylation levels of EGFR, Akt and Erk in 3D-COL were also enhanced by HB-EGF, they were much lower than those in TCPs (Fig. 5A).

The reduction of a cell response to HB-EGF in 3D-COL upon transient stimulation by sHB-EGF might be attributable to the reduced diffusion rate of sHB-EGF in the collagen gel. To test whether attenuation of EGFR signaling was characteristic of HB-EGF-dependent cell growth or due to the reduced diffusion, the activation states of Erk and Akt in cells grown in NCPs or 2D-agar were studied. In this case sHB-EGF would diffuse freely as it does in TCPs. Although Akt (Fig. 5B) or EGFR (data not shown) was

not reduced in NCPs or 2D-agar, steady states and sHB-EGF-induced phosphorylation levels of Erk and Akt in NCPs or 2D-agar were lower than those in TCPs, indicating that attenuation of EGFR signaling was not explained by the reduced diffusion rate of sHB-EGF (Fig. 5B).

Activation states of Erk and Akt were also examined under sustained cell culture conditions. For this assay, BRL-mock cells, BRL-HB cells and BRL cells expressing Raf-1, MEK1 and Akt1 were grown in TCPs or 3D-COL for 4 days in the presence of 10% FCS, and the phosphorylation levels of Erk and Akt were examined. The phosphorylation level of Erk in TCPs was much higher than that in 3D-COL regardless of the expression of HB-EGF or Raf-1, MEK1 and Akt1 (Fig. 5C). HB-EGF, or coexpression of Raf-1, MEK1 and Akt1, increased the phosphorylation level of Erk in 3D-COL, but the level was still lower than that of cells cultured in TCPs. This suggests a correlation between the phosphorylation level of Erk and the growth rate of BRL cells. The enhanced phosphorylation of Akt was also observed by expression of HB-EGF or coexpression of Raf-1, MEK1 and Akt1 in 3D-COL. This was consistent with results obtained using a transient assay (Fig. 5A), where expression of Erk and Akt in cells growing in 3D-COL was attenuated when compared with that in cells growing in TCPs. We observed that the phosphorylation level of Akt was reduced by expression of HB-EGF in TCPs, although the significance was not clarified.

We examined whether activation of the Raf-MEK-Erk and PI3K-Akt pathways is linked with cell cycle progression by evaluating cyclin D1 expression. BRL-mock cells showed reduced levels of cyclin D1 in 3D-COL compared with that in TCPs, suggesting that the cell cycle of BRL-mock cells in 3D-COL was arrested at G1 phase (Fig. 5C). Consistent with growth-promotion activity, HB-EGF or Raf, MEK and Akt increased cyclin D1 in 3D-COL to levels comparable with those in TCPs.

Finally, we examined EGFR downstream signaling in vivo. To determine the relationship of the activation state of EGFR signaling with HB-EGF dependency in cell growth, the phosphorylation levels of Erk and Akt of BRL-HB cells growing in tumors in mice were compared with those of BRL-HB cells growing in TCPs. The phosphorylation levels of Erk and Akt in tumors were lower than those of cells in TCPs (Fig. 5D), although the phosphorylation levels varied. Taken together, we conclude that the growth enhancement by HB-EGF was observed in culture conditions with lower levels of EGFR signaling compared with that seen in TCPs.

Integrin compensates for signals required for cell growth

Cell adhesion to the ECM substrate is mediated predominantly by integrins. Growth factor receptors and integrins activate some common signaling pathways (Schwartz and Ginsberg, 2002), and both signals cooperate functionally in a variety of biological processes. A previous study indicated that the expression level of EGFR is positively linked to that of integrin β1 and that both were crossregulated in 3D-LM (Wang et al., 1998). BRL cells mainly express β1 and β3 integrin subunits. Thus, we examined the levels of integrin β1 and integrin β3 proteins in BRL-mock cells grown in TCPs and 3D-COL. The integrin β1 levels in BRL-mock cells were significantly reduced when they were grown in 3D-COL compared with TCPs (Fig. 6A), whereas the levels of integrin β3 remained constant (data not shown). When HB-EGF was expressed in BRL cells, the level of integrin β1, particularly its mature form, was increased in cells grown in TCPs or 3D-COL. The combination of Raf-1 with MEK1 and Akt1 also consistently increased the

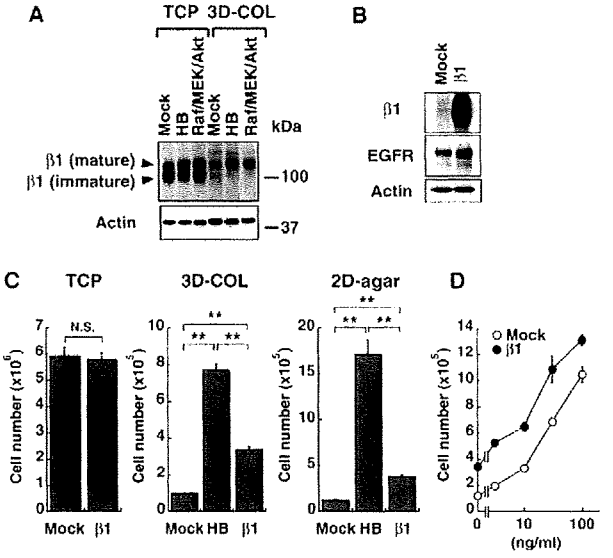

Fig. 6. Alteration of integrin β1 levels in various culture conditions. (A) Expression of integrin β1. BRL-mock cells, BRL-HB cells, or BRL cells expressing Raf-1, MEK1 and Akt1 were grown in TCPs or 3D-COL for 16 hours. The expression of integrin β1 was detected by immunoblotting. Actin was used as a loading control. (B) Expression of integrin β1 and EGFR in BRL-β1 cells. Expression of integrin β1 and EGFR in BRL-mock and BRL-β1 cells was detected using immunoblotting. Actin was used as a loading control. (C) Growth of BRL-β1 cells. BRL-mock, BRL-HB and BRL-β1 cells were cultured in TCPs for 4 days, in 3D-COL for 1 week or 2D-agar for 1 week. N.S., not significant; $^{**}P<0.01$. (D) Effect of recombinant sHB-EGF on growth of BRL-β1 cells. BRL-mock cells or BRL-β1 cells were cultured in 3D-COL for 1 week in the presence of indicated concentrations of recombinant sHB-EGF and 10% FCS.

integrin β1 levels under these culture conditions. We examined the level of integrin β1 of the BRL-HB cells growing in vivo and found that it was reduced in vivo compared with cells growing in TCPs (Fig. 5D). These results suggest that the integrin levels are linked with growth factor signaling in cells growing in 3D-COL or in vivo, as well as in 3D-LM.

To determine whether a reduced integrin β1 level in reduced cell adhesion conditions causes the diminished growth of BRL cells and their HB-EGF dependency, we established BRL cells expressing exogenous integrin β1 (BRL-β1) and examined cell growth in various culture conditions. Exogenous expression of integrin β1 resulted in an increased EGFR level (Fig. 6B). BRL-β1 cells grew faster than BRL-mock cells in 3D-COL or 2D-agar, but not in TCPs (Fig. 6C). However, cell growth rate induced by integrin β1 expression in 3D-COL or 2D-agar was slower than that induced by HB-EGF expression. Furthermore, when BRL-mock cells and BRL-β1 cells were stimulated with various concentrations of recombinant sHB-EGF in 3D-COL, BRL-β1 cells grew faster than BRL-mock cells in the same concentrations of sHB-EGF (Fig. 6D). However, the high concentration of sHB-EGF in BRL-mock cells far overcame the growth advantage of the BRL-β1 cells. These results suggest that a reduced integrin β1 level could partly cause the diminished growth of BRL cells and their HB-EGF dependency.

Integrins form stable focal contacts when cells are attached and spread to hard substrates, such as TCPs, with a corresponding

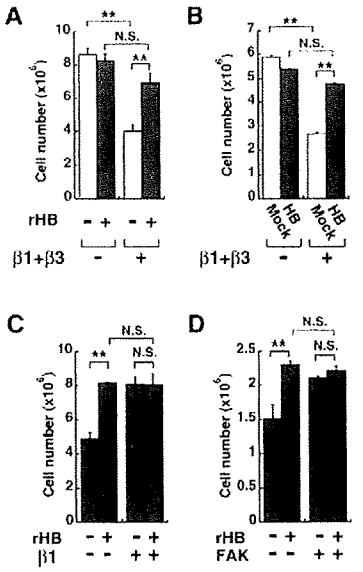

Fig. 7. HB-EGF dependency in cells cultured in reduced integrin conditions. (A) Effects of integrin antibodies on the growth of BRL cells in TCPs. BRL-mock cells stimulated with or without recombinant sHB-EGF (rHB; 30 ng/ml) were grown in the presence or absence of anti-integrin-β1 and anti-integrin-β3 antibodies (5 μg/ml each) in TCPs. (B) BRL-mock and BRL-HB cells were grown in the presence or absence of anti-integrin-β1 and anti-integrin-β3 antibodies (5 μg/ml each). (C) Effect of recombinant sHB-EGF on growth of integrin-β1-knockout cells in TCPs. Integrin-β1-knockout cells or integrin-β1-knockout cells expressing integrin β1 were cultured in the presence or absence of recombinant sHB-EGF (rHB; 30 ng/ml) in TCPs. (D) Effect of recombinant sHB-EGF on growth of FAK-knockout cells in TCPs. FAK-knockout cells or FAK-knockout cells expressing FAK were cultured in the presence or absence of recombinant sHB-EGF (rHB; 30 ng/ml) in TCPs. These cultures were maintained in the presence of 10% FCS. N.S., not significant; $^{**}P<0.01$.

generation of strong signals. By contrast, when cells are cultured on soft substrates, the formation of focal contacts is hampered, and integrin signals are reduced (Cukierman et al., 2001; Paszek et al., 2005). Although it is difficult to accurately estimate the strength of integrin signals directly, the morphology of cells cultured under various conditions (Fig. 2) and the phosphorylation levels of Erk and Akt in the absence of HB-EGF (Fig. 5) represent the strength of integrin signals within a particular cell culture system. Therefore, we speculated that, in combination with the expression level of integrin β1, integrin signals are strengthened in TCPs, whereas they are considerably decreased in 3D or 2D adhesion-reduced culture conditions.

We hypothesized that the integrin signal might predominantly contribute to promote cell growth in TCPs, thereby allowing the cells to grow without HB-EGF. However, integrin signals were too low to grow in cells cultured in 3D and 2D adhesion-reduced conditions, resulting in enhanced cell proliferation by HB-EGF. To test this hypothesis, we investigated the effect of integrin inhibition on HB-EGF dependency for cell growth in TCPs. First, BRL cells were cultured in the presence or absence of integrin antibodies. Although a single blockade of integrin β1 or integrin β3 scarcely inhibited the growth of BRL cells (data not shown), simultaneous blockade of integrins β1 and β3 suppressed the growth of BRL cells in TCPs (Fig. 7A). When sHB-EGF was added to the culture with the integrin antibodies, sHB-EGF almost recovered the growth rate to the level of BRL cells without the integrin antibodies, indicating that BRL cells exhibit HB-EGF-dependent growth in the presence of integrin antibodies. Growth stimulation by HB-EGF in TCPs was also shown upon comparison of the growth rate of BRL-mock and BRL-HB cells in the presence of integrin antibodies (Fig. 7B).

To further examine the contribution of integrin to cell growth in TCPs, we examined the HB-EGF dependency of cells obtained from an integrin-β1-knockout mouse. Fig. 7C shows that growth of cells lacking integrin β1 was HB-EGF-dependent in TCPs. Growth stimulation of integrin-β1-knockout cells was observed by addition of sHB-EGF to the medium. Reintroduction of integrin β1 increased the growth of integrin-β1-knockout cells in TCPs and induced the cells to become HB-EGF independent. These results indicate that the integrin system largely contributes to the growth of cells cultured in TCPs. FAK is a critical downstream effector of integrin signaling (Mitra and Schlaepfer, 2006). To further strengthen our hypothesis, we examined whether fibroblasts obtained from FAK-knockout mice ($MEF^{FAK-/-}$) showed HB-EGF dependency for growth in TCPs. Similarly to cases of integrin blockade with integrin antibodies (Fig. 7A,B) and integrin-β1-knockout cells (Fig. 7C), $MEF^{FAK-/-}$ cells exhibited HB-EGF-dependent growth in TCPs upon addition of sHB-EGF to the medium (Fig. 7D). Reintroduction of FAK increased the growth of FAK-knockout cells in TCPs, and the cells became less HB-EGF independent. Taken together, we conclude that integrin and HB-EGF share common signals for promoting cell growth, and that in TCPs integrins generate sufficient signals for growth, thereby contributing to the dispensability of HB-EGF for growth purposes. In 3D or 2D adhesion-reduced conditions the integrin signals are not sufficient to stimulate rapid cell growth, and therefore there is a cumulative contribution of integrins and growth factors toward cell growth.

3D culture facilitates growth-stimulatory activity of EGF, TGFα or ligands of other RTKs

We demonstrated here that growth stimulation by HB-EGF was facilitated in 3D culture systems or 2D cell adhesion-reduced conditions. To determine whether this feature was specific for HB-EGF or was a general feature of other growth factors, we tested the growth-stimulatory effects of various growth factors in TCPs and 3D-COL. None of the growth factors tested greatly enhanced cell growth of BRL-mock cells in TCPs. EGF and TGFα of the EGF family enhanced cell growth to the same extent as HB-EGF did in 3D-COL (Fig. 8). In addition, the growth of BRL cells in 3D-COL was enhanced by FGF-2 and IGF-1 and slightly enhanced by PDGF-BB (Fig. 8). These results indicate that culture conditions with reduced integrin signals also facilitated cell growth promotion by other members of the EGF family of growth factors or ligands of other RTKs.

Discussion

In this study, SKOV3 and BRL cells injected into nude mice exhibited HB-EGF-dependent growth; however, when these cells were cultured in TCPs, they displayed no HB-EGF dependency. Based on this finding, we investigated the effects of HB-EGF on cell growth under different culture conditions. Our results indicated the following: first, the HB-EGF dependency of cell growth was emphasized in culture systems in which cells grew in reduced cell-substrate adhesion, and this phenomenon was observed for transformed and non-transformed cells; second, the phosphorylation

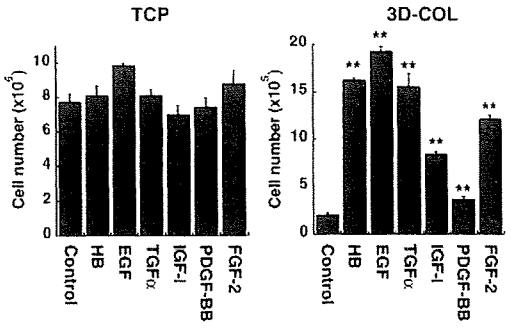

Fig. 8. Effect of EGF family growth factors or other RTK ligands on cell growth. BRL cells were cultured in the presence of EGF family growth factors (EGF, 5 ng/ml; HB-EGF, 50 ng/ml; TGFα, 5 ng/ml) or other growth factors (IGF-I, 50 ng/ml; PDGF-BB, 50 ng/ml; FGF-2, 50 ng/ml) in TCPs for 4 days or 3D-COL for 1 week in the presence of 10% FCS. $^{**}P<0.01$.

of Erk and Akt was drastically diminished in reduced cell-substrate adhesion conditions compared with that of TCPs, and therefore activation of Raf-MEK-Erk and PI3K-Akt pathways by HB-EGF or other growth factors is required for cell growth; third, the required signals for cell growth appeared to be produced by integrin in TCPs; and finally, monolayer cell culture in TCPs masked the growth-promoting activity of EGF, TGFα and ligands of other RTKs. To our knowledge, the present study is the first to examine the effects of EGFR ligands on cell growth under various culture conditions, using the same cell lines.

Reduced integrin signals emphasize growth-promotion activity of HB-EGF and other growth factors

Integrins are major players of cell adhesion to the ECM substrate. EGFR and integrins are thought to activate most common signaling pathways (Schwartz and Ginsberg, 2002). Here, we demonstrated that integrin signals largely affect EGFR-ligand-dependent cell growth. In the cases of cell-adhesion-reduced cultures (i.e. 3D-COL, 3D-LM, 3D-agar, 2D-agar and NCPs), integrin signals were reduced compared with that of TCPs, which was not sufficient to support cell growth. Under such conditions, the stimulation of EGFR by its ligands would be required for activation of downstream signaling molecules and promotion of cell growth. Coating of plastic surfaces of TCPs with poly-L-lysine reduces the integrin signal. HB-EGF stimulated SKOV3 cell growth in TCPs coated with poly-L-lysine (Yagi et al., 2005). Moreover, EGFR-expressing 32D and Ba/F3 cells show EGFR ligand-dependent growth in suspension culture. In addition, HB-EGF dependency was observed in the presence of the MEK inhibitor PD98059 in TCPs (Fig. 4B). These observations support our hypothesis that HB-EGF stimulates cell growth when integrin signals are reduced.

We have provided evidence that the activation states of EGFR and its downstream signaling molecules in TCPs differ from those in 3D-COL, NCPs and 2D-agar. The difference seems to be the level of signal strength rather than in signaling pathways. One critical difference is in the significant reduction in phosphorylation levels of EGFR, Erk and Akt in 3D-COL compared with TCPs, before and after HB-EGF stimulation. The reduced level of phosphorylation could explain why PD98059 prevented cell growth more effectively in 3D-COL than in TCPs (Fig. 4B). Decreased phosphorylation levels of EGFR, Erk and Akt might be partially due to the reduced level of EGFR and Akt protein levels. Since the protein levels of Akt (Fig. 5B) and EGFR (data not shown) were not reduced in NCPs or 2D-agar, this might not be the major cause of attenuation of the activation state of EGFR and downstream signaling molecules. Our results also suggest that robust stimulation of EGFR ligands is required for cells to maintain their growth potential in growth-suppressive conditions used for the present study compared with TCPs. HB-EGF dependency could thus be preferentially observed in cells in reduced cell-adhesion conditions.

We have provided evidence that the integrin β1 level was reduced in 3D-COL compared with that of TCPs, and that the expression of HB-EGF or the simultaneous expression of Raf-1, MEK1 and Akt1 increased integrin β1 expression (Fig. 6A). Consistently, previous studies showed that EGFR inhibition reduced integrin β1 levels, and vice versa, in mammary carcinoma cells cultured with 3D-LM (Wang et al., 1998). These results imply that reduction of integrin and EGFR in 3D culture systems might be partly responsible for HB-EGF dependency.

Integrins are enhanced and/or required for growth factor signaling (Streuli and Akhtar, 2009). In the present study, we showed that HB-EGF-dependent growth was observed under integrin-reduced conditions. This does not deny the requirement of integrins in growth-factor-dependent cell growth. In fact, we showed here that overexpression of integrin β1 in BRL cells resulted in enhanced cell growth in 3D-COL and 2D-agar (Fig. 6C,D). In the culture conditions tested in this study (i.e. anti-integrin antibodies, integrin-β1-knockout cells and FAK-knockout cells), integrin signals might have been partially inhibited. Complete inhibition of integrin signals might cause cell growth arrest or cell death, even in the presence of growth factors.

Application for development of molecular targets of cancer therapy

Colony formation in semisolid media, also known as anchorage-independent growth, is a hallmark of oncogenic transformation in vitro (Hanahan and Weinberg, 2000). Formation of 'foci', which are aberrantly accumulated cell masses seen in TCPs, is another criterion for oncogenic transformation of cells. Although these criteria of oncogenic transformation are well reflected in the tumorigenicities of cancer cells in vivo, the reason why oncogenic cells exhibit such transformed characters in vitro is not completely understood. The present study sheds light on these characteristics of transformed cells. It will be possible to consider tumor formation of cancer cells in vivo as a type of 3D growth. Focus formation, as well as colony formation in semisolid media, requires the ability to grow in 3D. As shown here, HB-EGF or other growth factors are required for cell growth in 3D or 2D integrin-signal-impeded conditions, therefore normal cells do not grow under such culture conditions in the absence of exogenously added growth factors. By contrast, transformed cells could be activated by signaling via Erk and Akt pathways, or by mutations in or overexpression of EGFR, Ras or other signaling molecules. This could result in the acquisition of cell proliferation ability in integrin-signal-impeded conditions in the absence of exogenously added growth factors, although cell proliferation could be enhanced if growth factors, such as HB-EGF, are exogenously provided. In this context, the requirement of cell adhesion for growth in normal cells or 'anchorage dependency' should be taken as meaning the requirement of growth-promoting signals stimulated by cell adhesion, rather than just adhesion of the cell to a substrate.

EGFR systems and their downstream signaling molecules are promising targets for cancer treatment. Actually, many EGFR inhibitors and EGFR-targeted antibodies are currently being used in the clinic or being assessed in clinical trials (Hynes and Lane, 2005; Mosesson and Yarden, 2004). As shown in the present study, the cell growth potential of EGFR ligands is not well documented in TCPs, whereas 3D or 2D integrin-signal-impeded conditions demonstrate this efficiently and reflect the tumorigenicity of nude mice. CRM197, an inhibitor of HB-EGF, strongly inhibited tumor formation by ovarian cancer cells in nude mice (Miyamoto et al., 2004) and HB-EGF-induced cell growth in 3D-COL, but this effect was not detected in cells grown in TCPs (supplementary material Fig. S4). Thus, 3D cultures or culture systems that impede integrin signals might be a better model for the evaluation of inhibitors that target the EGFR system and its downstream signaling molecules. The present study also suggested that EGFR-ligand-induced cells and oncogenic-transformed cells share a common feature in terms of their 3D growth potential. Therefore, the identification of molecules that are specifically required for growth in 3D environments could result in the development of novel targets for cancer therapy. Such molecules might not be required for the normal functioning of epithelial cells that are grown in monolayers. Therefore, therapeutics that target such molecules could inhibit tumor cells without adverse toxicity and side effects. Further studies on molecules that facilitate cell growth in 3D and 2D integrin-signal-impeded culture systems might provide novel molecular targets for cancer therapy.

Materials and Methods

Antibodies and reagents

The anti-HB-EGF extracellular domain antibody and recombinant sHB-EGF, EGF and TGFα were obtained from R&D Systems. The anti-HB-EGF C-terminal domain and anti-EGFR antibodies were from Santa Cruz Biotechnology. The anti-Erk, anti-phosphoErk (T202/Y204), anti-Akt, anti-phospho-Akt (S473) and anti-phospho-EGFR (Y845, Y992 and Y1068) antibodies were from Cell Signaling Technology. The anti-actin and anti-integrin-β1 cytoplasmic domain antibodies were from Chemicon. The function-blocking antibodies against integrins β1 (Ha2/5) and β3 (2C9.G2) were from PharMingen. The anti-cyclin-D1 antibody (DCS-6) was from Medical & Biological Laboratories. ZD1839 was a gift from AstraZeneca, and the other kinase inhibitors were from Calbiochem. Recombinant IGF-1, PDGF-BB and FGF-2 were from PeproTech. CRM197 was prepared as described previously (Miyamoto et al., 2004).

Cells and culture

SKOV3 cells and SKOV3 cells expressing human HB-EGF or small-hairpin RNAs for human HB-EGF were established as described previously (Miyamoto et al., 2004). Buffalo rat liver (BRL) and ecotropic retrovirus packaging Plat-E (Morita et al., 2000) cells were gifts from Kaoru Miyazaki (Yokohama City University, Japan) and Toshio Kitamura (The University of Tokyo, Japan), respectively. FAK-null cells (Ilic et al., 1995) were obtained from Tsuyoshi Akagi (KAN Research Institute, Japan) with the permission of Michinari Hamaguchi (Nagoya University, Japan). Integrin-β1-null GE11 cells (Gimond et al., 1999) and GE11 cells expressing integrin β1 were obtained from Kiyotoshi Sekiguchi with the permission of Reinhard Fässler (Max-Planck Institute for Biochemistry, Germany). All cells, except for MCF-10A cells, were maintained in DMEM supplemented with 10% FCS, penicillin and streptomycin. MCF-10A cells obtained from ATCC were maintained with mammary epithelial cell basal medium (MEBM; Clonetics), containing bovine pituitary extract (13 μg/ml), insulin (5 μg/ml), EGF (5 ng/ml), hydrocortisone (2 μg/ml) and cholera toxin (100 ng/ml). FCS-free cultures were grown in DMEM supplemented with insulin (5 μg/ml), transferrin (5 μg/ml), sodium selenite (5 ng/ml), penicillin and streptomycin.

Retrovirus vectors and infection

The retrovirus vectors pCX4pur and pCX4bsr (Akagi et al., 2003) were gifts from T. Akagi (KAN Research Institute, Japan). The pCX4hyg and pCX4zeo vectors were constructed by substituting the puromycin-resistance gene of pCX4pur with hygromycin-resistance and zeocin-resistance genes, respectively. Wild-type and uncleavable mutant human HB-EGF cDNAs were cloned into pCX4pur as previously described (Wang et al., 2006). The mutant HB-EGF was characterized previously (Miyamoto et al., 2004). The cDNAs for constitutively active Raf-1 and MEK1 were described previously (Umata et al., 2001). The cDNAs for wild-type and constitutively active Akt1 were gifts from Michiyuki Matsuda (Kyoto University, Japan) with the permission of Yukiko Gotoh (The University of Tokyo, Japan). The cDNAs for wild-type Raf-1 and MEK1, which were obtained from Makoto Tsuneoka (Takasaki University of Health and Welfare, Japan), were fused with an HA tag using an HA-tagging vector (Wang et al., 2006), and then subcloned into pCX4zeo and pCX4hyg, respectively. The cDNA of human integrin β1A was obtained from Junichi Takagi (Osaka University, Japan) with the permission of Yoshikazu Takada (University of California, Davis, CA). A FAK cDNA derived from BRL cells was obtained by reverse transcription-PCR and cloned into the *Bam*HI-*Not*I sites of the pCX4bsr vector using the following primers: 5′-CAGGATCCACCATGGCAGCTGCTTATCTTG-3′ (forward) and 5′-CTGCGGCCGCTCAGTGTGGCCGTGTCTGCC-3′ (reverse). Retrovirus infection was performed as described previously (Wang et al., 2006). A mixed population of cells was used to avoid clonal effects.

Samples for immunoblotting

Cells grown in culture dishes were lysed with 50 mM Tris-HCl (pH 7.4), 150 mM NaCl, 1% (w/v) NP-40, 0.1 mM Na_3VO_4, 1 mM NaF, 10 mM sodium pyrophosphate, 10 mM β-glycerophosphate, 10 mM *o*-phenanthroline and protease inhibitor cocktail (Nacalai Tesque). Cells grown in collagen gels were lysed with a 2× concentration of lysis buffer. The cell lysates were centrifuged and concentrated with ice-cold trichloroacetic acid. Tumors were snap frozen with liquid nitrogen and lysed with the lysis buffer using a Polytron homogenizer (Kinematica).

Tumor-formation assay

Tumor-formation assays were performed as described previously (Wang et al., 2006). The handling of animals was performed in accordance with the guidelines prescribed by Osaka University (Osaka, Japan).

Collagen gel cultures

Ice-cold bovine type I collagen (Nitta Gelatin; 3 mg/ml), reconstitution buffer comprising 2.2% (w/v) $NaHCO_3$, 0.2 M HEPES and 50 mM NaOH, 10× DMEM-F12 (1:1) medium and cells suspended in serum-free DMEM (5×10^6 cells/ml) were mixed in an 8:1:1:0.1 ratio and poured into 24-well dishes (0.5 ml/well). After a 30-minute incubation at 37°C, the gels were overlaid with 1 ml DMEM containing 15% FCS and incubated for 1 week. The collagen gels were incubated with 0.5 ml of 0.5% (w/v) bacterial collagenase (Gibco) in HBS (+) (comprising 10 mM HEPES pH 7.3, 140 mM NaCl, 4 mM KCl, 1.8 mM $CaCl_2$ and 1 mM $MgCl_2$) at 37°C until they dissolved, and the cells were then harvested by centrifugation. The cells were resuspended in PBS (–) containing 0.1% (w/v) BSA and 20 mM EDTA, and counted under a microscope. All experiments were carried out in triplicate, and the data were presented as the mean ± s.d.

Matrigel cultures

Cells were mixed with ice-cold 12.3 mg/ml Matrigel (Becton Dickinson; 1.7×10^5 cells/ml) and poured into 24-well dishes (0.3 ml/well). After a 30-minute incubation at 37°C, the gels were overlaid with 1 ml DMEM containing 10% FCS and incubated for 4 days. MCF-10A cells were cultured for 1 week in the presence of hydrocortisone (1 μg/ml), insulin (5 μg/ml) and cholera toxin (100 ng/ml). The gels were incubated with 0.5 ml of 2000 U/ml dispase (Godo Shusei) in HBS (+) at 37°C until they dissolved, and the cells were then harvested by centrifugation. All experiments were carried out in triplicate, and the data were presented as the mean ± s.d.

Semisolid media cultures

Bottom-layer agarose (0.5%; 4 ml) was overlaid with top-layer agarose (0.33%; 3 ml) containing 1×10^4 cells. The numbers of colonies with diameters greater than 0.2 mm were counted under a dissecting microscope after 4 weeks of culture. For the cell-counting experiments, the cells were cultured with DMEM containing 1.5% (w/v) methylcellulose, and then recovered by centrifugation after diluting the medium with ice-cold PBS (–). All experiments were carried out in triplicate, and the data were presented as the mean ± s.d. The semisolid media cultures performed in this study were carried out in the presence of 10% FCS.

Cultures using fine-structured surface culture plates

Cells (1×10^4) suspended in DMEM containing 3% FCS were plated on NCPs (Scivax), and cultured for 3 days. All experiments were carried out in triplicate, and the data were presented as the mean ± s.d.

Evaluation of cell growth in various conditions

Upregulation ratio, which represents HB-EGF dependency for cell growth, was calculated using the following equation: doubling time of BRL-HB cells/doubling time of BRL-mock cells.

Statistical analysis

Statistical significance was determined by Student's *t*-test and ANOVA for a single pair of conditions and multiple pair of conditions, respectively, with a value of $P<0.02$ considered statistically significant.

We thank T. Akagi, K. Miyazaki, T. Kitamura, M. Hamaguchi, R. Fässler, K. Sekiguchi, M. Matsuda, Y. Gotoh, J. Takagi and M. Tsuneoka

for providing cell lines, vectors and cDNA. We also thank H. Hanafusa, T. Akagi, J. Takagi and K. Sekiguchi for their useful comments regarding this work. This work was supported by Grants-in-Aid from the Ministry of Education, Culture, Sports, Science, and Technology (14032202 and 16207014 to E.M.) and the Charitable Trust Osaka Cancer Research-Fund (to H.M.).

Reference

Akagi, T., Sasai, K. and Hanafusa, H. (2003). Refractory nature of normal human diploid fibroblasts with respect to oncogene-mediated transformation. *Proc. Natl. Acad. Sci. USA* **100**, 13567-13572.

Cao, L., Yao, Y., Lee, V., Kiani, C., Spaner, D., Lin, Z., Zhang, Y., Adams, M. E. and Yang, B. B. (2000). Epidermal growth factor induces cell cycle arrest and apoptosis of squamous carcinoma cells through reduction of cell adhesion. *J. Cell Biochem.* **77**, 569-583.

Cukierman, E., Pankov, R., Stevens, D. R. and Yamada, K. M. (2001). Taking cell-matrix adhesions to the third dimension. *Science* **294**, 1708-1712.

Fan, Z., Lu, Y., Wu, X., DeBlasio, A., Koff, A. and Mendelsohn, J. (1995). Prolonged induction of p21Cip1/WAF1/CDK2/PCNA complex by epidermal growth factor receptor activation mediates ligand-induced A431 cell growth inhibition. *J. Cell Biol.* **131**, 235-242.

Fu, S., Bottoli, I., Goller, M. and Vogt, P. K. (1999). Heparin-binding epidermal growth factor-like growth factor, a v-Jun target gene, induces oncogenic transformation. *Proc. Natl. Acad. Sci. USA* **96**, 5716-5721.

Gimond, C., van Der Flier, A., van Delft, S., Brakebusch, C., Kuikman, I., Collard, J. G., Fässler, R. and Sonnenberg, A. (1999). Induction of cell scattering by expression of β1 integrins in β1-deficient epithelial cells requires activation of members of the rho family of GTPases and downregulation of cadherin and catenin function. *J. Cell Biol.* **147**, 1325-1340.

Goishi, K., Higashiyama, S., Klagsbrun, M., Nakano, N., Umata, T., Ishikawa, M., Mekada, E. and Taniguchi, N. (1995). Phorbol ester induces the rapid processing of cell surface heparin-binding EGF-like growth factor: conversion from juxtacrine to paracrine growth factor activity. *Mol. Biol. Cell* **6**, 967-980.

Hanahan, D. and Weinberg, R. A. (2000). The hallmarks of cancer. *Cell* **100**, 57-70.

Harding, P. A., Davis-Fleischer, K. M., Crissman-Combs, M. A., Miller, M. T., Brigstock, D. R. and Besner, G. E. (1999). Induction of anchorage independent growth by heparin-binding EGF-like growth factor (HB-EGF). *Growth Factors* **17**, 49-61.

Hashimoto, K., Higashiyama, S., Asada, H., Hashimura, E., Kobayashi, T., Sudo, K., Nakagawa, T., Damm, D., Yoshikawa, K. and Taniguchi, N. (1994). Heparin-binding epidermal growth factor-like growth factor is an autocrine growth factor for human keratinocytes. *J. Biol. Chem.* **269**, 20060-20066.

Higashiyama, S., Abraham, J. A., Miller, J., Fiddes, J. C. and Klagsbrun, M. (1991). A heparin-binding growth factor secreted by macrophage-like cells that is related to EGF. *Science* **251**, 936-939.

Higashiyama, S., Iwamoto, R., Goishi, K., Raab, G., Taniguchi, N., Klagsbrun, M. and Mekada, E. (1995). The membrane protein CD9/DRAP 27 potentiates the juxtacrine growth factor activity of the membrane-anchored heparin-binding EGF-like growth factor. *J. Cell Biol.* **128**, 929-938.

Ho, R., Minturn, J. E., Hishiki, T., Zhao, H., Wang, Q., Cnaan, A., Maris, J., Evans, A. E. and Brodeur, G. M. (2005). Proliferation of human neuroblastomas mediated by the epidermal growth factor receptor. *Cancer Res.* **65**, 9868-9875.

Hynes, N. E. and Lane, H. A. (2005). ERBB receptors and cancer: the complexity of targeted inhibitors. *Nat. Rev. Cancer* **5**, 341-354.

Ilic, D., Furuta, Y., Kanazawa, S., Takeda, N., Sobue, K., Nakatsuji, N., Nomura, S., Fujimoto, J., Okada, M. and Yamamoto, T. (1995). Reduced cell motility and enhanced focal adhesion contact formation in cells from FAK-deficient mice. *Nature* **377**, 539-544.

Iwamoto, R., Handa, K. and Mekada, E. (1999). Contact-dependent growth inhibition and apoptosis of epidermal growth factor (EGF) receptor-expressing cells by the membrane-anchored heparin-binding EGF-like growth factor. *J. Biol. Chem.* **274**, 7260-7272.

Lee, G. Y., Kenny, P. A., Lee, E. H. and Bissell, M. J. (2007). Three-dimensional culture models of normal and malignant breast epithelial cells. *Nat. Methods* **4**, 359-365.

Lembach, K. J. (1976). Induction of human fibroblast proliferation by epidermal growth factor (EGF): enhancement by an EGF-binding arginine esterase and by ascorbate. *Proc. Natl. Acad. Sci. USA* **73**, 183-187.

Lynch, T. J., Bell, D. W., Sordella, R., Gurubhagavatula, S., Okimoto, R. A., Brannigan, B. W., Harris, P. L., Haserlat, S. M., Supko, J. G., Haluska, F. G. et al. (2004). Activating mutations in the epidermal growth factor receptor underlying responsiveness of non-small-cell lung cancer to gefitinib. *N. Engl. J. Med.* **350**, 2129-2139.

Massagué, J. and Pandiella, A. (1993). Membrane-anchored growth factors. *Annu. Rev. Biochem.* **62**, 515-541.

Mitra, S. K. and Schlaepfer, D. D. (2006). Integrin-regulated FAK-Src signaling in normal and cancer cells. *Curr. Opin. Cell Biol.* **18**, 516-523.

Miyamoto, S., Hirata, M., Yamazaki, A., Kageyama, T., Hasuwa, H., Mizushima, H., Tanaka, Y., Yagi, H., Sonoda, K., Kai, M. et al. (2004). Heparin-binding EGF-like growth factor is a promising target for ovarian cancer therapy. *Cancer Res.* **64**, 5720-5727.

Morita, S., Kojima, T. and Kitamura, T. (2000). Plat-E: an efficient and stable system for transient packaging of retroviruses. *Gene Ther.* **7**, 1063-1066.

Mosesson, Y. and Yarden, Y. (2004). Oncogenic growth factor receptors: implications for signal transduction therapy. *Semin. Cancer Biol.* **14**, 262-270.

Normanno, N., De Luca, A., Bianco, C., Strizzi, L., Mancino, M., Maiello, M. R., Carotenuto, A., De Feo, G., Caponigro, F. and Salomon, D. S. (2006). Epidermal growth factor receptor (EGFR) signaling in cancer. *Gene* **366**, 2-16.

Ongusaha, P. P., Kwak, J. C., Zwible, A. J., Macip, S., Higashiyama, S., Taniguchi, N., Fang, L. and Lee, S. W. (2004). HB-EGF is a potent inducer of tumor growth and angiogenesis. *Cancer Res.* **64**, 5283-5290.

Osborne, C. K., Hamilton, B., Titus, G. and Livingston, R. B. (1980). Epidermal growth factor stimulation of human breast cancer cells in culture. *Cancer Res.* **40**, 2361-2366.

Paszek, M. J., Zahir, N., Johnson, K. R., Lakins, J. N., Rozenberg, G. I., Gefen, A., Reinhart-King, C. A., Margulies, S. S., Dembo, M., Boettiger, D. et al. (2005). Tensional homeostasis and the malignant phenotype. *Cancer Cell* **8**, 241-254.

Pierce, J. H., Ruggiero, M., Fleming, T. P., Di Fiore, P. P., Greenberger, J. S., Varticovski, L., Schlessinger, J., Rovera, G. and Aaronson, S. A. (1988). Signal transduction through the EGF receptor transfected in IL-3-dependent hematopoietic cells. *Science* **239**, 628-631.

Rheinwald, J. G. and Green, H. (1977). Epidermal growth factor and the multiplication of cultured human epidermal keratinocytes. *Nature* **265**, 421-424.

Schmeichel, K. L. and Bissell, M. J. (2003). Modeling tissue-specific signaling and organ function in three dimensions. *J. Cell Sci.* **116**, 2377-2388.

Schwartz, M. A. and Ginsberg, M. H. (2002). Networks and crosstalk: integrin signalling spreads. *Nat. Cell Biol.* **4**, E65-E68.

Streuli, C. H. and Akhtar, N. (2009). Signal co-operation between integrins and other receptor systems. *Biochem. J.* **418**, 491-506.

Wang, F., Weaver, V. M., Petersen, O. W., Larabell, C. A., Dedhar, S., Briand, P., Lupu, R. and Bissell, M. J. (1998). Reciprocal interactions between β1-integrin and epidermal growth factor receptor in three-dimensional basement membrane breast cultures: a different perspective in epithelial biology. *Proc. Natl. Acad. Sci. USA* **95**, 14821-14826.

Wang, X., Mizushima, H., Adachi, S., Ohishi, M., Iwamoto, R. and Mekada, E. (2006). Cytoplasmic domain phosphorylation of heparin-binding EGF-like growth factor. *Cell Struct. Funct.* **31**, 15-27.

Weaver, V. M., Petersen, O. W., Wang, F., Larabell, C. A., Briand, P., Damsky, C. and Bissell, M. J. (1997). Reversion of the malignant phenotype of human breast cells in three-dimensional culture and in vivo by integrin blocking antibodies. *J. Cell Biol.* **137**, 231-245.

Yagi, H., Miyamoto, S., Tanaka, Y., Sonoda, K., Kobayashi, H., Kishikawa, T., Iwamoto, R., Mekada, E. and Nakano, H. (2005). Clinical significance of heparin-binding epidermal growth factor-like growth factor in peritoneal fluid of ovarian cancer. *Br. J. Cancer* **92**, 1737-1745.

Yamada, K. M. and Cukierman, E. (2007). Modeling tissue morphogenesis and cancer in 3D. *Cell* **130**, 601-610.

Yamazaki, S., Iwamoto, R., Saeki, K., Asakura, M., Takashima, S., Yamazaki, A., Kimura, R., Mizushima, H., Moribe, H., Higashiyama, S. et al. (2003). Mice with defects in HB-EGF ectodomain shedding show severe developmental abnormalities. *J. Cell Biol.* **163**, 469-475.

Yu, X., Sharma, K. D., Takahashi, T., Iwamoto, R. and Mekada, E. (2002). Ligand-independent dimer formation of epidermal growth factor receptor (EGFR) is a step separable from ligand-induced EGFR signaling. *Mol. Biol. Cell* **13**, 2547-2557.

PATTERNS & PHENOTYPES

HB-EGF Decelerates Cell Proliferation Synergistically With TGFα in Perinatal Distal Lung Development

Seigo Minami, Ryo Iwamoto,* and Eisuke Mekada

Heparin-binding epidermal growth factor-like growth factor (HB-EGF) is a member of the EGF family of growth factors that is suggested to be involved in distal lung development. In HB-EGF null ($HB^{del/del}$) newborns, a histopathologic analysis revealed abnormally thick saccular walls occurring from embryonic day 18.5 that reduced the terminal saccular space area. HB-EGF gene deletion resulted in a significant increase in cell proliferation, indicating that HB-EGF suppresses distal lung cell proliferation. Furthermore, an analysis of saccular morphology and proliferation in HB-EGF and transforming growth factor-α (TGFα) double-mutant newborns revealed that HB-EGF and TGFα function synergistically in this suppression. Finally, crosses between $HB^{del/del}$ mice and waved 2 mice, a hypomorphic EGF receptor (EGFR) mutant strain, suggest that HB-EGF and EGFR cooperate in this process. Thus, HB-EGF has a novel suppressive function that contributes to decelerating distal lung cell proliferation synergistically with TGFα through EGFR in perinatal distal lung development. ***Developmental Dynamics 237:247–258, 2008.***

Key words: HB-EGF; TGFα; EGFR; distal lung development

Accepted 4 November 2007

INTRODUCTION

In the mouse embryo, the development of the lung begins with the outpouching of an endodermal budding from the foregut at embryonic day (E) 9–9.5 (E9–E9.5). Mouse lung development comprises six different stages: the organogenesis (E9.5–E12), the pseudoglandular stage (E12–E16.5), the canalicular stage (E16.5–E17.5), the saccular stage (E17.5 to postnatal day 4 [P4]), the alveolization phase (P4–P14), and the phase of microvascular maturation (P14–P21) (Ten Have-Opbroek, 1991; Burri, 1999; Roth-Kleiner et al., 2004). The progression from canalicular to saccular stage is especially important for lung development, as terminal sacs and vascularization develop during the canalicular stage. Subsequently, the number of terminal sacs and vascularization rapidly increases in the saccular stage. In this stage, as interstitial tissue thins, the saccular spaces expand, the capillary network forms, and type I and II epithelial cells differentiate. Therefore, the saccular stage, which prepares the distal lung for subsequent alveolarization and

ABBREVIATIONS E embryonic day **P** postnatal day **EGF** epidermal growth factor **EGFR** EGF receptor **HB-EGF** heparin-binding EGF-like growth factor **TGFα** transforming growth factor-α **AR** amphiregulin **EPR** epiregulin **BTC** betacellulin **GAPDH** glyceraldehydes-3-phosphate dehydrogenase **PBS** phosphate-buffered saline **PCR** polymerase chain reaction **RT-PCR** reverse transcription-PCR **TSSA** terminal saccular space area **TUNEL** terminal deoxynucleotidyltransferase-mediated dUTP nick-end labeling **DAB** diaminobenzidine.

Department of Cell Biology, Research Institute for Microbial Diseases, Osaka University, Osaka, Japan
Grant sponsor: the Ministry of Education, Culture, Sports, Science, and Technology; Grant number: 18570176; Grant number: 18370079; Grant sponsor: Takeda Science Foundation.
***Correspondence to: Ryo Iwamoto, Department of Cell Biology, Research Institute for Microbial Diseases, Osaka University, 3-1, Yamadaoka, Suita, Osaka 565-0871, Japan. E-mail: riwamoto@biken.osaka-u.ac.jp**

DOI 10.1002/dvdy.21398
Published online 10 December 2007 in Wiley InterScience (www.interscience.wiley.com).

gas exchange upon parturition, is absolutely critical for normal lung development.

In normal lung development, epidermal growth factor receptor (EGFR) signaling is fundamentally established. EGFR null mice exhibit defective branching morphogenesis and saccular formation as well as immature differentiation of type II epithelial cells. These EGFR null mice die within a few days after birth, most likely due to respiratory failure caused by immature lung development (Miettinen et al., 1995, 1997; Sibilia and Wagner, 1995). Such molecular genetic studies demonstrate that EGFR signaling plays a crucial role during the saccular stage of lung development.

However, EGFR signaling is complex. The EGF-ErbB signaling network includes four related tyrosine kinase receptors, EGFR (ErbB1) and the ErbB receptors (ErbB2–4), and it also includes multiple ligands of the EGF/neuregulin superfamily (Holbro and Hynes, 2004). The EGF family ligands that bind to EGFR include EGF, transforming growth factor-α (TGFα), amphiregulin (AR), epiregulin (EPR), betacellulin (BTC), epigen, and heparin-binding EGF-like growth factor (HB-EGF) (Harris et al., 2003).

HB-EGF binds to and activates both EGFR and ErbB4 (Higashiyama et al., 1991; Elenius et al., 1997). HB-EGF is synthesized as a type I transmembrane protein (proHB-EGF), and as other EGF family ligands (Massague and Pandiella, 1993), proHB-EGF is cleaved at the juxtamembrane domain, resulting in the shedding of soluble HB-EGF (sHB-EGF; Goishi et al., 1995). sHB-EGF is a potent mitogen and chemoattractant for several cell types (Raab and Klagsbrun, 1997), while proHB-EGF acts as a juxtacrine growth factor that signals to adjacent neighboring cells in a nondiffusible manner (Iwamoto and Mekada, 2000).

HB-EGF has been implicated in several physiological and pathological processes (Raab and Klagsbrun, 1997). Importantly, analyses of HB-EGF null mice have shown that HB-EGF is a crucial factor for proper heart development and function (Iwamoto et al., 2003; Jackson et al., 2003; Yamazaki et al., 2003; Iwamoto and Mekada, 2006), eyelid development (Mine et al., 2005), skin wounding healing (Shirakata et al., 2005), and skin hyperplasia (Kimura et al., 2005). Notably, HB-EGF has been suggested to be involved in proper lung development, as HB-EGF null newborns exhibit saccular wall thickening, a decrease in the number of sacculi, and the immature differentiation of type II epithelial cells (Jackson et al., 2003). Still, a detailed understanding of the key mechanisms underlying such lung abnormalities remains unclear.

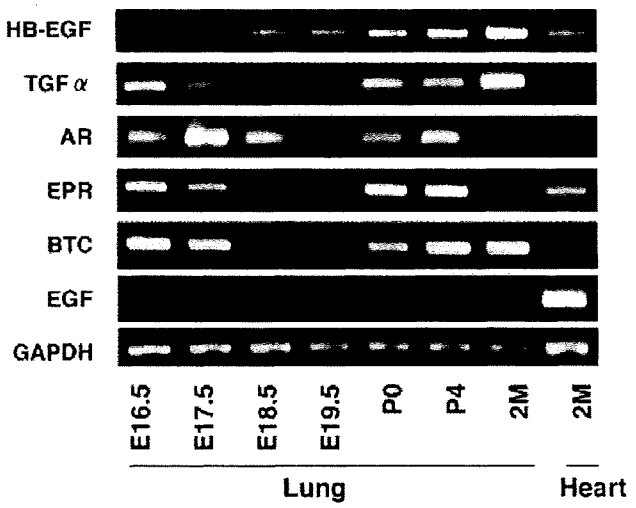

Fig. 1. Chronological analysis of EGFR ligands mRNA expression. RT-PCR of HB-EGF, TGFα, AR, EPR, BTC, EGF, and GAPDH mRNAs from mouse lung at the indicated stages (E16.5–adult) and heart (adult) was performed. For abbreviations, see list.

Therefore, to ascertain how HB-EGF regulates normal lung development, we used HB-EGF null mice to investigate how this specific EGFR ligand regulates cell proliferation in developing pulmonary tissue. Here, we present a novel mechanistic function for HB-EGF in saccular formation. Our data suggest that HB-EGF decelerates cell proliferation synergistically with TGFα selectively through EGFR signaling in perinatal distal lung development.

RESULTS

Postnatal Early Lethality of $HB^{del/del}$ Mice With C57BL/6J Background

We previously reported that approximately half of $HB^{del/del}$ mice with a mixed background (C57BL/6J, ICR, and CBA) show early lethality within a few weeks after birth. The survivors reach adulthood, but many gradually die around 2 to 3 months after birth, probably from heart failure (Iwamoto et al., 2003). In this study, however, we found that the $HB^{del/del}$ mice that have been back-crossed for more than eight generations onto a background of C57BL/6J strain almost all died within a few days after birth and rarely grew up (Fig. S1). No significant difference between $HB^{del/del}$ and $HB^{+/+}$ newborns was noted in body weight ($HB^{del/del}$: 1.42 ± 0.07 g, n = 7 vs. $HB^{+/+}$: 1.38 ± 0.05 g, n = 8; P = 0.67). Although we did not find any abnormalities in our $HB^{del/del}$ lungs with the mixed background of C57BL/6J, ICR and CBA, it has been reported that HB-EGF null mice with the mixed background of C57BL/6J and 129/Sv strains exhibit developmental abnormality in lung (Jackson et al., 2003). We did not detect any obvious histological abnormalities in lung development during pseudoglandular and canalicular stages with the $HB^{del/del}$ mice in C57BL/6J background (data not shown). These observations suggest that any developmental abnormality in lung occurring during the perinatal stage might be a major cause of the perinatal lethality of our $HB^{del/del}$ mice with C57BL/6J background. Therefore, we investigate here the HB-EGF function in lung development, especially focusing on the

perinatal saccular stage, by using $HB^{del/del}$ mice with a C57BL/6J background.

HB-EGF Expression Is Sustained During Prenatal Saccular Stage

First, we performed a chronological analysis of mRNA expression of EGFR ligands including HB-EGF in the lung during canalicular to perinatal saccular stage by reverse transcription-polymerase chain reaction (RT-PCR; Fig. 1). All of the EGFR ligands except EGF have already commenced expression by E16.5. At this stage, however, HB-EGF expression was extremely low when compared with the other EGFR ligands. Expressions of TGFα, AR, EPR, and BTC decreased markedly from E18.5 to E19.5, while only HB-EGF expression was sustained and gradually increased during this stage. Subsequently, expression of all the EGFR ligands except for EGF were increased rapidly just after birth. These chronological expression profiles of EGFR ligands suggest that only HB-EGF is a major factor among EGFR ligands in the developing prenatal lung.

HB-EGF Is Expressed in Lung Alveolar Epithelial Cells

To examine the expression pattern of HB-EGF in lung development, a targeting vector containing the *LacZ* reporter gene for HB-EGF expression was used (Iwamoto et al., 2003). *LacZ*-positive cells were detected in a manner of scattered distributions both in epithelial and interstitial cells of $HB^{del/+}$ and $HB^{del/del}$ newborns and $HB^{del/+}$ adult lungs (Fig. 2). Vascular endothelial cells (as indicated in Fig. 2B) and large bronchial epithelial cells (data not shown) were negative for *LacZ* detection. Although RT-PCR analysis showed HB-EGF expression in lung of the canalicular stage (Fig. 1), we could not detect *LacZ*-positive cells clearly in lung sections of prenatal embryos (data not shown). This disparity might be due to less sensitivity of *LacZ*-staining to that of RT-PCR. The observed pattern of HB-EGF expression in lung suggests that HB-EGF may participate in lung saccular and alveolar development and maintenance of mature lung formation.

Lungs Lacking HB-EGF Exhibit Abnormally Thickened Morphology in Saccular Walls During Saccular Stage

Therefore, to investigate the role of HB-EGF in distal lung development, we examined the morphology of distal lungs in $HB^{del/del}$ embryos and newborns during the saccular stage. $HB^{del/del}$ lungs exhibited an abnormally thickened morphology in saccular walls, an increased number of cells in the saccular septae, and poorly inflated sacculi in parts when compared with wild-type lungs (Fig. 3A). These abnormalities were observed in more than half of the newborn $HB^{del/del}$ lungs. Although $HB^{del/del}$ mice are known to exhibit enlarged cardiac valves and cardiac hypertrophy, these lung phenotypes were obviously not caused by pulmonary edema due to severe heart failure, based on the following observations; first, saccular septae were not edematous histologically. Second, no significant difference between $HB^{del/del}$ and $HB^{+/+}$ lungs were found in wet-to-dry lung weight ratio ($HB^{del/del}$: 5.32 ± 0.23, n = 7 vs. $HB^{+/+}$: 5.63 ± 0.15, n = 8; $P = 0.27$).

To analyze quantitatively these developmental abnormalities in $HB^{del/del}$ lungs, the terminal saccular space areas (TSSA) were measured (Shi et al., 1999; Zhao et al., 2001; Yu et al., 2004). In this analysis, a decrease of TSSA represents an increase of thickness of saccular walls and/or a decrease of saccular inflation. As a result, TSSA was significantly reduced in $HB^{del/del}$ lungs at E18.5, E19.5, and postnatal day (P) 0, but not at E17.5, when compared with those of wild-type lungs at each stage (Fig. 3B). Thus, the abnormalities in $HB^{del/del}$ lung saccular morphology occurred from E18.5 and were remarkable especially at birth (Fig. 3B). These results indicate that HB-EGF is involved in normal distal lung formation during the perinatal saccular stage.

Although it has been reported that the HB-EGF null lung presents an immature differentiation in sacculi (Jackson et al., 2003), our immunohistochemical analysis revealed no remarkable change in the expression of pro-surfactant protein C, a marker for the differentiated type II epithelial cells, between $HB^{+/+}$ and $HB^{del/del}$ lung sacculi (Fig. 4), suggesting that the observed abnormality in lung sacculi of our $HB^{del/del}$ mice is not due to defects in differentiation of saccular epithelium.

HB-EGF Contributes to Deceleration of the Distal Lung Cell Proliferation

Next, we examined whether the thickening of the saccular walls in $HB^{del/del}$ lungs is due to an increased proliferation or to a reduced apoptosis of the distal lung cells. Thus, cell proliferation and apoptosis in distal lungs during perinatal saccular were examined by immunohistochemistry of Ki67, a proliferation marker, and terminal deoxynucleotidyltransferase-mediated dUTP nick-end labeling (TUNEL) staining, respectively.

In distal lungs of E19.5 $HB^{del/del}$ embryos, a significantly increased number of Ki67-positive cells was detected compared with wild-type (Fig. 5A). Consistent with the TSSA analysis (Fig. 3B), in each stage of E18.5 to P0, the ratio of Ki67-positive cells to total cells was significantly increased in $HB^{del/del}$ lung, compared with that of wild-type (Fig. 5B). Moreover, while in the wild-type lung the ratio of Ki67-positive cells had gradually decreased during the perinatal saccular stage, in $HB^{del/del}$ lungs the higher ratio of Ki67-positive cells remained until E19.5 (Fig. 5B). On the other hand, only a few TUNEL-positive cells were detected both in wild-type and $HB^{del/del}$ lungs during this stage, and there was no significant difference in the ratio of TUNEL-positive cells to total cells between wild-type and $HB^{del/del}$ lungs (Fig. 5C,D). These results indicate that abnormally thickened saccular walls in $HB^{del/del}$ lungs is due to increased proliferation, but not to reduced apoptosis, in the distal lung cells and that HB-EGF contributes to the deceleration of such distal lung cell proliferation.

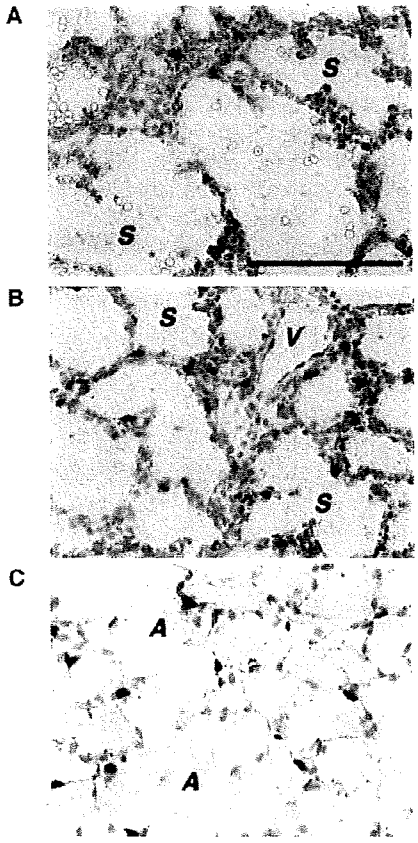

Fig. 2. HB-EGF expression in newborn lung sacculi. *LacZ* staining of (A) $HB^{del/+}$ newborn lung, (B) $HB^{del/del}$ newborn lung, and (C) $HB^{del/+}$ 2-month-old lung. The *LacZ*-stained tissues were counterstained with nuclear fast red. Original magnification: ×400. V, vessel; S, sacculus; A, alveolus. For other abbreviations, see list. Scale bar = 100 μm.

HB-EGF Functions Synergistically With TGFα in Perinatal Distal Lung Development

Recently, we have reported on the synergistic functions of HB-EGF and TGFα in the mouse eyelid closure pro-

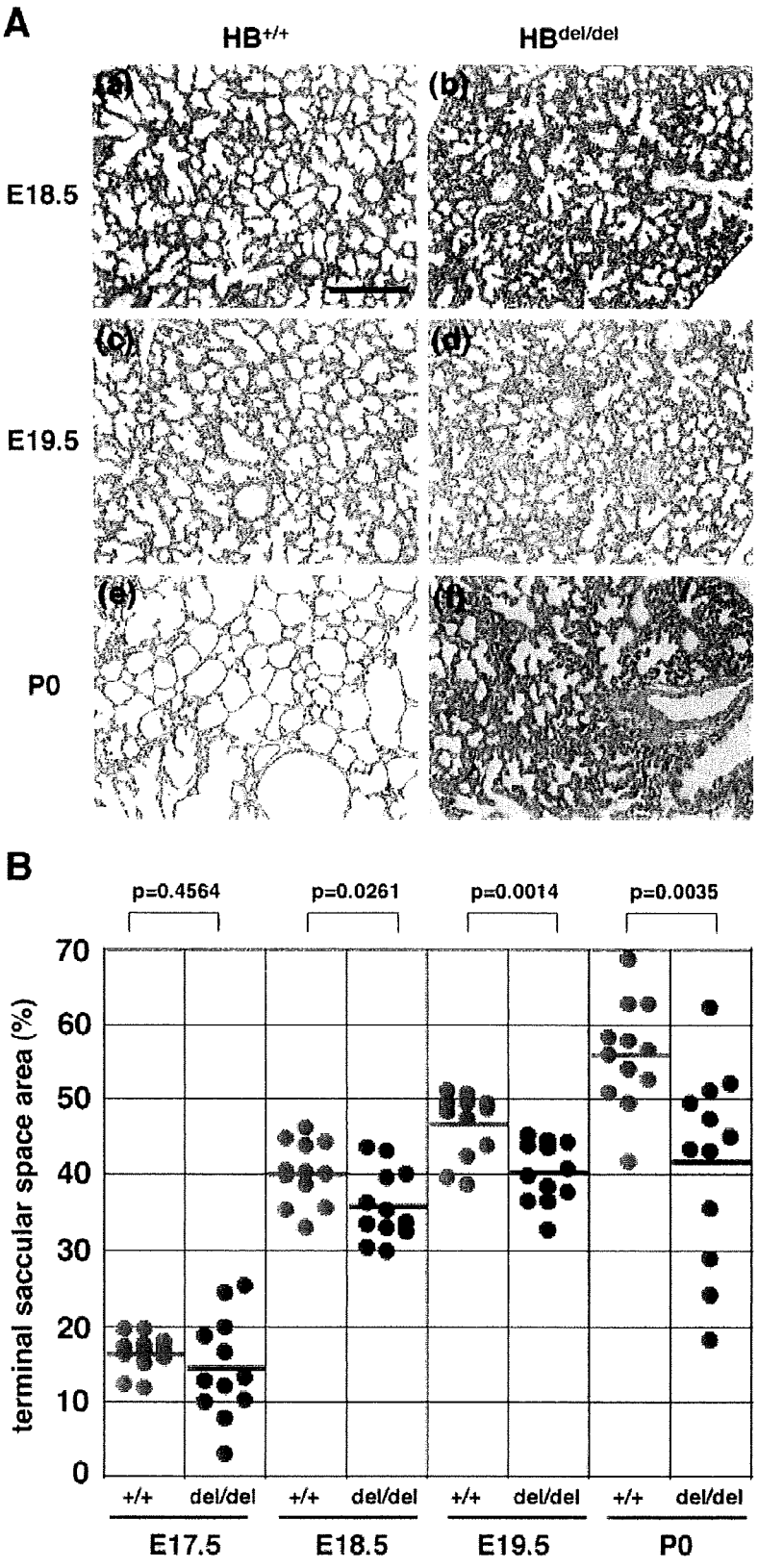

Fig. 3.

Fig. 3. Comparison of embryonic and newborn pup lung morphology between $HB^{del/del}$ and $HB^{+/+}$ genotypes. **A:** Representative hematoxylin/eosin-stained sections of lungs from $HB^{+/+}$(a,c,e) and $HB^{del/del}$ (b,d,f) at E18.5 (a,b), E19.5 (c,d), and newborn (P0) (e,f). **B:**Comparison of TSSA of $HB^{del/del}$ and $HB^{+/+}$ lungs. Each dot represents the percentage of TSSA from a single embryo or a newborn pup, with the horizontal lines representing the mean value for each genotype (n = 12). For abbreviations, see list. Original magnification, ×100. Scale bar = 200 μm in A.

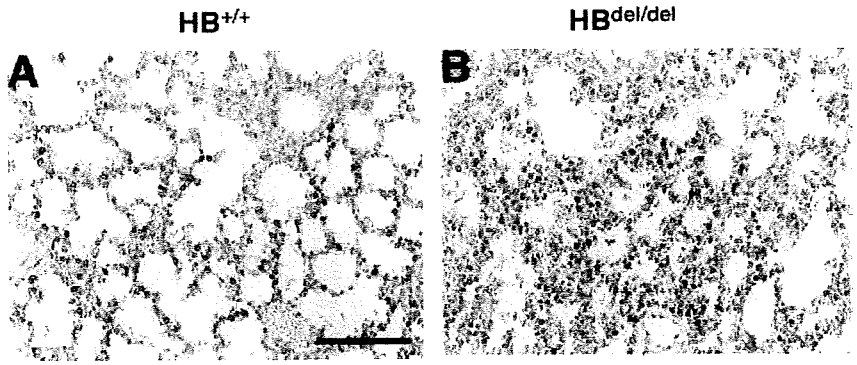

Fig. 4. Immunohistochemistry for pro-surfactant protein C. **A,B:** Sections of $HB^{+/+}$ (A) and $HB^{del/del}$ (B) newborn lung sacculi were immunostained for pro-SpC, a marker for type II epithelial cells. For abbreviations, see list. Original magnification, ×200. Scale bar = 100 μm.

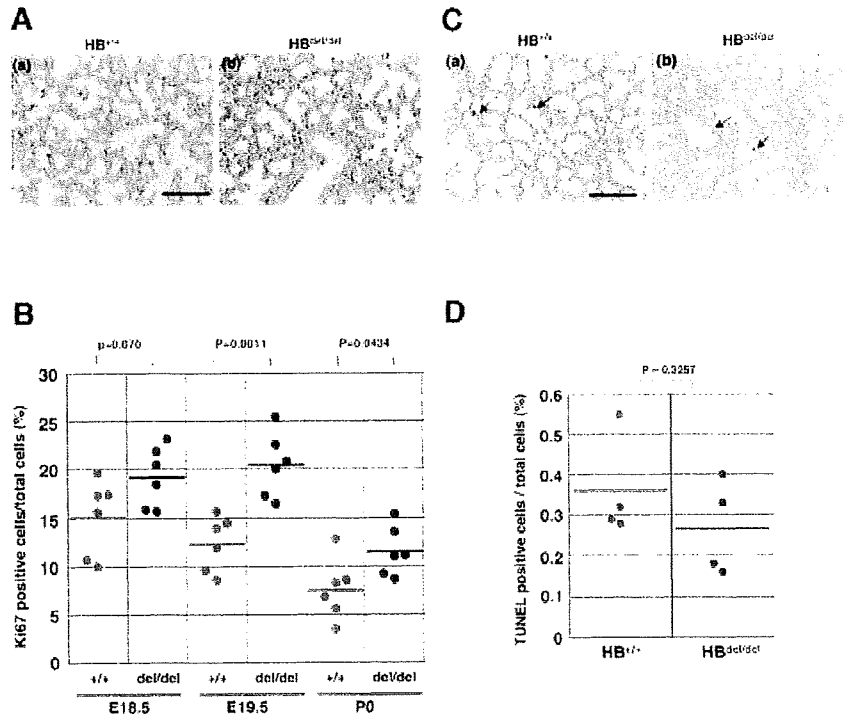

Fig. 5. Comparison of cell proliferation and apoptosis in embryonic and newborn pup lungs from $HB^{del/del}$ and $HB^{+/+}$ genotypes. **A:** Representative sections of $HB^{+/+}$ (a) and $HB^{del/del}$ (b) lungs at E19.5 immunostained for Ki67. **B:** Comparison of percentage of Ki67-positive cells in total lung cells at E18.5, E19.5, and newborn (P0). Each dot represents the percentage of Ki67-positive cells/total cells from a single embryo or a newborn pup, with the horizontal lines representing the mean value for each genotype (n = 6). **C:** Representative TUNEL-stained sections of $HB^{+/+}$ (a) and $HB^{del/del}$ (b) lungs at E19.5. Arrows indicate TUNEL-positive cells. **D:** Comparison of TUNEL-positive cell in lung saccular cells at E19.5. Each dot represents the percentage of TUNEL-positive cells/total cells from a single embryo, with the horizontal lines representing the mean value for each genotype (n = 4). For abbreviations, see list. Original magnification, ×200. Scale bar = 100 μm in A,C.

cess (Mine et al., 2005). Although lung abnormalities have not been reported in TGFα null mice to date, conditional prenatal overexpression of TGFα resulted in abnormal lung morphology at birth (Kramer et al., 2007), suggesting that proper expression of TGFα in lung is important for normal perinatal lung development.

As the expression of TGFα is regulated by HB-EGF in an autocrine manner in keratinocytes (Hashimoto et al., 1994; Piepkorn et al., 1998), we examined whether the defects in lung saccular development in $HB^{del/del}$ lungs were affected by changes in TGFα expression level. Major changes in the level of TGFα expression were not detected between wild-type and $HB^{del/del}$ lungs; however, the level of TGFα might even be somewhat slightly higher in the $HB^{del/del}$ lungs. Likewise, no significant difference was detected in the level of HB-EGF expression between wild-type and $TGF\alpha^{-/-}$ lungs (Fig. S2).

To test for a functional relationship between HB-EGF and TGFα in perinatal lung development, we examined double-null mutants of TGFα and HB-EGF. We tried to breed HB-EGF and TGFα double-null mice; however, intercrosses of $HB^{del/+}$; $Tgf\alpha^{+/-}$ double-heterozygous male and female mice could not produce any $HB^{del/del}$; $Tgf\alpha^{-/-}$ homozygous double-null newborns (in total 260 newborns from 39 litters). Thus, we compared $HB^{del/del}$; $Tgf\alpha^{+/+}$ and $HB^{+/+}$; $Tgf\alpha^{-/-}$ single homozygous null lungs with $HB^{del/del}$; $Tgf\alpha^{+/-}$ and $HB^{del/+}$; $Tgf\alpha^{-/-}$ lungs, respectively, of newborns. First, the TSSA in $Tgf\alpha^{-/-}$ single null lungs was significantly reduced compared with that of wild-type (Fig. 6A,B), indicating that TGFα also contributes to perinatal distal lung development. Then, TSSA was significantly reduced in $HB^{del/del}$; $Tgf\alpha^{+/-}$ lungs compared with $HB^{del/del}$; $Tgf\alpha^{+/+}$ lungs (Fig. 6A,B). On the other hand, TSSA in $HB^{del/+}$; $Tgf\alpha^{-/-}$ lungs was reduced slightly compared with $HB^{+/+}$; $Tgf\alpha^{-/-}$ lungs, without statistical significance. Scattering profiles of TSSA suggest that these differences were due to the increased penetrance, rather than severity, of the TSSA reduction.

Then, regarding proliferation rate of the distal lung cells, the ratio of Ki67-positive cells to the total cells was significantly increased in $HB^{del/del}$; $Tgf\alpha^{+/-}$ and $HB^{del/+}$; $Tgf\alpha^{-/-}$ lungs compared with $HB^{del/del}$; $Tgf\alpha^{+/+}$ and $HB^{+/+}$; $Tgf\alpha^{-/-}$ lungs, respectively. $HB^{+/+}$; $Tgf\alpha^{-/-}$ single null lungs also showed higher ratio of Ki67-positive cells than that of $HB^{+/+}$; $Tgf\alpha^{+/+}$ wild-type lungs, although not statistically significant (Fig. 6C,D).

These results strongly suggest that TGFα also contributes to deceleration of the distal lung cells in a relatively weaker manner than HB-EGF, and